J Appl Physiol (1985). 2018 Dec 1; 125(6): 1944–1967. PMCID: PMC64
Published online 2018 Sep 20. PMID: 302
doi: 10.1152/japplphysiol.00095.2018: 10.1152/japplphysiol.00095.2018
Vascular Aging

Computational model-based assessment of baroreflex function fro response to Valsalva maneuver

Samuel A. Kosinski,[1] Brian E. Carlson,[1] Scott L. Hummel,[2,3] Robert D. Brook,[2] and Daniel A. Beard[1]

[1]Molecular and Integrative Physiology, University of Michigan, Ann Arbor, Michigan
[2]Internal Medicine and Cardiology, University of Michigan, Ann Arbor, Michigan
[3]Ann Arbor Veterans Affairs Health System, Ann Arbor, Michigan
Corresponding author.
Address for reprint requests and other correspondence: D. A. Beard, 2800 Plymouth Rd., Ann Arbor, MI 4810
mail: beardda@umich.edu).

Received 2018 Jan 31; Revised 2018 Aug 6; Accepted 2018 Sep 14.

Abstract

Functional metrics of autonomic control of heart rate, including baroreflex sensitivity, have been show be strongly associated with cardiovascular risk. A decrease in baroreflex sensitivity with aging is hypothesized to represent a contributing causal factor in the etiology of primary hypertension. To asse baroreflex function in human subjects, two complementary methods to simulate the response in heart elicited by the Valsalva maneuver were developed and applied to data obtained from a cohort of healtl normal volunteers. The first method is based on representing the baroreflex arc as a simple linear filte transforming changes in arterial pressure to changes in R-R interval. The second method invokes a physiologically based model for arterial mechanics, afferent baroreceptor strain-dependent firing, and control of heart rate via central autonomic response to changes in afferent inputs from aortic and carot sensors. Analysis based on the linear filter model reveals that the effective response time of the barore arc tends to increase with age in healthy subjects and that the response time/response rate is a predicto resting systolic pressure. Similar trends were obtained based on the physiologically based model. Ana of the Valsalva response using the physiologically based model further reveals that different afferent i from the carotid sinus and the aortic arch baroreceptors govern different parts of the heart rate respons The observed relationship between baroreflex sensitivity and systolic pressure is surprising because hypertensive subjects were excluded from the study, and there was no observed relationship between arterial pressure and age.

NEW & NOTEWORTHY We introduce two methods to assess baroreflex function from data record from human subjects performing the Valsalva maneuver. Results demonstrate that the baroreflex respo

time tends to increase with age in healthy subjects, that response time represents a predictor of resting systolic pressure, and that the Valsalva response reveals different effects mediated by baroreceptors in carotid sinus compared with those in the aortic arch.

Keywords: baroreflex, computational physiology, Valsalva

INTRODUCTION

Stretch receptors in the walls of the aortic arch and the carotid sinus fire in response to changes in arte wall strain, sending signals that are interpreted by the central nervous system to influence the firing of sympathetic and parasympathetic efferent fibers via the arterial baroreflex system. Increases in arterial pressure, resulting in increased wall strain, result in decreases in heart rate through increased parasympathetic and decreased sympathetic tone. Conversely, a drop in pressure results in an increase sympathetically and parasympathetically mediated heart rate. The sensitivity of the baroreflex system, measured as the change in heart rate elicited by a given change in arterial pressure, has been shown to an effective predictor of cardiovascular disease/mortality (16, 17). Predictive relationships between baroreflex sensitivity (BRS) and various metrics of cardiovascular function (ejection fraction, pulmon wedge pressure, and cardiac work capacity) have been observed (17). BRS has also proven useful in assessing pathophysiological mechanisms underlying orthostatic hypotension (20, 24).

Dysfunction of the baroreflex system has been associated with hypertension in humans. A relationship between increased sympathetic outflow and decreased BRS has been observed in some hypertensive patients (10). An association between BRS and responsiveness to renal denervation therapy in resistar hypertension (36) points to a potential role of the baroreflex system in the etiology of neurogenic hypertension. Indeed, studies by Thrasher (33) demonstrate that surgically induced unloading of arteri baroreceptors causes neurogenic hypertension in animal models. Our theoretical studies support the hypothesis that vascular mechanical remodeling (stiffening of large arteries), resulting in a resetting of baroreflex strain sensitivity, represents a root cause of primary hypertension (2–4, 6, 27).

Baroreflex responsiveness may be assessed by measuring either the direct response of peripheral sympathetic outflow or the heart rate to changes in arterial pressure (29). The present study focuses or autonomic reflex control of heart rate. A variety of experimental procedures have been applied to pert pressure and assay a reflex response in heart rate. These approaches include administration of vasodila and vasoconstrictors such as α-agonists and angiotensin (5, 8, 16, 17). In addition to using pharmacological approaches to alter pressure, early studies required invasive indwelling catheters to measure arterial pressure on a beat-to-beat basis (5, 16, 17). Imholz et al. (14) introduced use of Valsa maneuver as a noninvasive stimulus and use of finger arterial pressure monitoring for noninvasive pre measurement. Moreover, just as there exist a variety of approaches to acutely perturb and measure pre to elicit a response in heart rate, numerous approaches have been applied to analyze the resulting data 18, 26). One approach is to estimate the slope of the change in R-R interval versus some measure of arterial pressure. Related definitions of BRS include the slope of the change in R-R interval versus the change in systolic pressure measured over the previous R-R interval (16, 17), the slope of the change R-R interval versus the systolic pressure measured two beats before a given R-R interval (5), and the s of R-R interval versus the systolic pressure measured from the previous beat (15). There is some ambiguity in all of these definitions as they are applied to a time window that is not necessarily clearly

defined. For example, Kautzner et al. refer to a “period of interest…selected by the operator” (15). Th also exist methods of analyzing spontaneous fluctuations that are not subject to influence by choice of protocol or operator bias (23, 26, 35). For example, Westerhof et al. (35) compute the gain as the cros correlation between R-R interval and systolic pressure at a fixed delay found to show the greatest posi correlation.

The goals of this study are to develop and characterize alternate methods to analyze autonomic reflexe involved in arterial pressure and heart rate dynamics, to apply these methods to data obtained from hu subjects undergoing a Valsalva maneuver, and to use computational modeling to improve our understanding of the physiological response to the Valsalva maneuver. We have developed two complementary methods to analyze data on arterial pressure and heart rate that are equivalently and robustly applicable analyzing spontaneous fluctuations as well as larger responses elicited by physiolc perturbations (e.g., tilt and Valsalva). Both methods are applied to data obtained using a device for noninvasive measurement of arterial blood pressure (Finometer; Finapres Medical Systems) before, during, and after a Valsalva maneuver in a small cohort of normotensive subjects (14 female, 13 male) ranging in age from 21 to 67 yr. The first method uses a simple linear filter to transform input time co data on arterial pressure to output time courses of heart rate and R-R interval. This method invokes a minimal number of adjustable parameters representing a gain, an offset, and a time constant. The seco method uses a mathematical model based on representing physiological mechanisms (4). The physiologically based model invokes additional parameters representing processes associated with art mechanics, baroreceptor afferent firing response to arterial strain, and heart rate response to changes i afferent firing. The two methods yield different (related and potentially complementary) metrics of baroreflex sensitivity.

Analysis of data from normotensive subjects reveals *1*) no statistically discernable differences betwee functional parameters estimated for the female versus male participants; *2*) an increase in baroreflex response time with increasing age; and *3*) a significant relationship between baroreflex function and systolic pressure, with faster responsiveness associated with lower pressure. Furthermore, analysis usi the physiologically mechanistic model reveals new insight into features of the Valsalva response, with different inputs from aorta versus carotid sinus dominating different parts of the response. The observ relationship between baroreflex sensitivity and systolic pressure is surprising because hypertensive subjects were excluded from the study, and there was no observed relationship between arterial pressu and age.

METHODS

Data Collection

Healthy subjects (14 female, 13 male) were recruited with exclusion criteria of arterial hypertension, h disease, history positive for vascular surgery, pulmonary hypertension, aneurism, dissection, stroke, thromboembolism, valvular disease, inherited cardiomyopathy, or connective tissue disease. This investigation was approved by the University of Michigan Institutional Review Board. Written inform consent was obtained from all study participants.

The Valsalva maneuver was utilized to examine blood pressure and heart rate dynamics over a known

period of baroreflex activation, while minimizing risk and discomfort for human subjects (19, 30). Subjects performed an ~15-s Valsalva maneuver by bearing down on a closed pipe and mouthpiece fit with a pressure transducer, to obtain airway pressure. Subjects were asked to maintain a target airway pressure of ~30–40 mmHg. Recorded airway pressure was then employed as an approximate measure intrathoracic pressure in the analysis described below.

To collect heart rate and arterial pressure data before, during, and after the Valsalva maneuver, a finge arterial pressure monitoring device (Finometer; Finapres Medical Systems) was used to collect a continuous time series of arterial blood pressure and interbeat heart rate through a finger cuff (14, 25). Finometer directly measures peripheral arterial pressure at the finger cuff while the device provides ar estimation of central arterial blood pressure. Measurements were obtained from subjects positioned in supine manner throughout data collection. Baseline blood pressure and heart rate metrics were collect for 10–15 s, followed by a Valsalva maneuver of consistent airway pressure for another 10–20 s. This duration ensures baroreflex response while minimizing the influences of other reflex responses, such a through chemoreceptors (9). Normal baroreflex thresholds have been outlined as at least 30 mmHg fo least 7 s (21), but these benchmarks may not apply to hypertensive individuals with potential barorefle dysfunction, as they have not been substantiated in nonnormal subjects. Not all subjects participating this study were able to reach such thresholds, but that does not necessarily limit the impact of Valsalva circulatory dynamics.

Time courses of airway pressure, arterial pressure, and heart rate for a typical subject (*subject 4*, fema yr) are shown in Fig. 1. Before the initiation of the Valsalva, heart rate and mean arterial pressures fluctuate around baseline of ~75 mmHg and 60 min^{-1}. The four distinct phases of the physiological response to the Valsalva maneuver are identified (12) as follows.

Phase 1. The rapid increase in thoracic pressure (beginning at time t = 15.5 s) causes a transient incre in pressure, due to increased transmural pressure on the great veins, the heart, and the large arteries in thoracic cavity. In this example, the arterial pressure during the Valsalva period peaks near time t = 17 This rapid increase in pressure elicits a transient drop in heart rate, which achieves a local minimum a time t = 18 s.

Phase 2. After the initial peak in pressure, the effect of increased transmural pressure on restricting fl to the large veins causes a decrease in stroke volume (reflected in a decrease in pulse pressure) and associated drop in mean arterial pressure. Heart rate increases to compensate for this drop in pressure, by the end of the Valsalva period, heart rate has reached a peak of ~92 min^{-1} in this example. The inc in heart rate that occurs during the Valsalva period can bring about a partial or complete restoration in arterial pressure. [The restoration phase has been distinguished as phase 2b (34).]

Phase 3. When the Valsalva is released (when expiratory pressure drops back to normal baseline), the a rapid drop in pressure, because preload drops and there is a delay in refilling the large veins that wer squeezed during the Valsalva. This drop in pressure may be associated with a second peak in heart rat occurring at t = 34 s in this example.

Phase 4. When preload is restored, and while heart rate remains elevated, there can be an overshoot i pressure response, with a local peak in systolic and mean pressure occurring after the release of the Valsalva. This transient increase in pressure is associated with a transient decrease in heart rate, which

to 57 min^{-1} at t = 39 s for this subject. Eventually, the pressures and heart rate restore to their baseline values.

The degree to which individual features described above are pronounced varies from subject to subject. Not all features are detectable in all recordings from all subjects, as discussed below.

Linear Filter Model

We represent the influence of changes in arterial wall strain on heart rate using a simple linear filter governed by the following equation

$$\tau \frac{\mathrm{dRR}\,(t)}{\mathrm{d}t} = \alpha P_p\,(t) + R_o - \mathrm{RR}\,(t) \quad (1$$

where RR(t) is the R-R interval (heart rate = 1/RR), $P_p(t)$ is the pulse pressure, and α, R_o, and τ are adjustable parameters. Since afferent baroreceptor fibers fire in response to changes in strain, this mod assumes that changes in pulse pressure affect changes in heart rate. The parameter α represents the gai whereas the time constant τ determines how quickly the system responds to changes in pressure. Assu a piecewise constant right-hand side of *Eq. 1* over an individual beat of duration Δt, *Eq. 1* has the solu

$$\mathrm{RR}\,(t) = \mathrm{RR}\,(t-\Delta t)\,e^{-\Delta t/\tau} + \left(1 - e^{-\Delta t/\tau}\right)\left[\alpha P_p\,(t-\Delta t) + R_o\right] \quad (2$$

The linear filter model is fit to measured data by adjusting the parameters α, R_o, and τ for each subject match the recorded RR(t) to the time series predicted by *Eq. 2*.

Physiologically Based Model

To simulate the physiological processes underlying the baroreflex response, we adapt the baroreflex component of model of Beard et al. (4), which simulates pressure-dependent arterial strain, strain-dependent afferent baroreceptor firing, and the influence of afferent input on the heart rate.

A simple viscoelastic model is used to simulate arterial wall dynamics

$$\mu \frac{\mathrm{d}D}{\mathrm{d}t} = \frac{DP}{2} - kD(D - D_o)^2 \quad (3$$

where D is the vessel diameter and P is the pressure drop across the wall of the vessel. *Equation 3* ass a parabolic steady-state pressure-diameter relationship. The parameter μ represents an effective viscos of the vessel wall, and k and D_o determine the stiffness of the vessel. Figure 2 shows data from Stefan et al. (32) used to parameterize the arterial mechanics model of *Eq. 3*. Figure 2*A* shows aortic pressure

measured in a control subject, and Fig. 2*B* shows the recorded pressure-diameter loop for the cardiac cycle. Using the measured pressure as an input to the model, the model-predicted pressure-diameter lo matched to the measured data in Fig. 2*B*, obtained with parameter values μ = 2.1 s·mmHg, $k = 0.505$ mmHg/mm^2, and $D_o = 12.35$ mm. These parameter values are held fixed for the model-based analysis described below. To equivalently represent vessels of different sizes, we introduce a scaled version of [3]

$$\mu \dot{d} = \frac{1}{2} dP - k' d(d - D')^2$$

where $d = D/D_{\text{ref}}$, $D' = D_o/D_{\text{ref}}$, $k' = kD_{\text{ref}}^2$, and D_{ref} is a reference diameter. For the aorta, usi $D_{\text{ref}} = 20$ mm, the scaled mechanics parameters become $k' = 202$ mmHg and $D' = 0.617$. Furthermore, simulate the different strains experienced by vessels inside the thoracic cavity (including the aortic arc and those outside (including carotids), we invoke two versions of this vessel model

$$\mu \dot{d}_1 = \frac{1}{2} d_1 \left[P_A(t) - P_{\text{th}}(t)\right] - k' d_1 (d_1 - D')^2$$

$$\mu \dot{d}_2 = \frac{1}{2} d_2 P_A(t) - k' d_2 (d_2 - D')^2 \quad (4$$

where $P_A(t)$ is the arterial pressure and $P_{\text{th}}(t)$ is the intrathoracic pressure. The nondimensional diame represents relative aortic diameter, and d_2 represents the relative (nondimensional) diameter of the carotids. The model assumes that the baroreceptors in each compartment sense the dynamic strain rela to mean strain computed as the running average

$$\frac{\mathrm{d}\overline{\varepsilon_1}}{\mathrm{d}t} = \left(d_1 - \overline{\varepsilon_1}\right)/\tau_s$$

$$\frac{\mathrm{d}\overline{\varepsilon_2}}{\mathrm{d}t} = \left(d_2 - \overline{\varepsilon_2}\right)/\tau_s \quad (5$$

where τ_s is a time constant related to baroreceptor adaptation. The value of this parameter controls ho quickly the system adapts to chronic changes in mean pressure, and thus its value does not influence t responses observed over the timescales analyzed here. The instantaneous relative strains are compared

with the running averages to compute response functions that are nonzero only when instantaneous stı exceeds the running average

$$\delta_{\varepsilon 1} = \max\left(d_1 - \overline{\varepsilon_1}, 0\right)$$

$$\delta_{\varepsilon 2} = \max\left(d_2 - \overline{\varepsilon_2}, 0\right) \quad (6$$

The afferent baroreceptor firing rates, f_{BR1} and f_{BR2}, are related to $\delta_{\varepsilon 1}$ and $\delta_{\varepsilon 2}$ by the saturable relationships

$$f_{BR1} = f_0 s_1 \frac{\delta_{\varepsilon 1}}{\delta_{\varepsilon 1} + \delta_{\varepsilon 0}}$$

$$f_{BR2} = f_0 s_2 \frac{\delta_{\varepsilon 2}}{\delta_{\varepsilon 2} + \delta_{\varepsilon 0}} \quad (7$$

where f_0 and $\delta_{\varepsilon 0}$ are parameters defining baroreceptor gain and saturation and s_1 and s_2 represent the fraction of baroreceptor afferents in firing-permissive states. The quantities s_1 and s_2 are governed by

$$\frac{ds_1}{dt} = a\left(1 - s_1\right) - b s_1 \frac{\delta_{\varepsilon 1}}{\delta_{\varepsilon 1} + \delta_{\varepsilon 0}}$$

$$\frac{ds_2}{dt} = a\left(1 - s_2\right) - b s_2 \frac{\delta_{\varepsilon 2}}{\delta_{\varepsilon 2} + \delta_{\varepsilon 0}} \quad (8$$

where a and b are rates of baroreceptor activation and deactivation. Parameters τ_s, $\delta_{\varepsilon 0}$, f_0, a, and b we previously estimated on the basis of measurements following step changes in nonpulsatile carotid pres and ramping pulsatile aortic pressures in vivo (4). The model assumes that sympathetic tone, represen by variable $\phi_{SN}(t)$, is governed by the following equation

$$\frac{d\phi_{SN}}{dt} = f_{SN}\left(1 - \phi_{SN}\right) - f_1\left[2g f_{BR1} + 2\left(1 - g\right) f_{BR2}\right]\phi_{SN} \quad (9$$

where f_{SN} and f_1 are model parameters pertaining to autonomic tone and firing rate and g determines t fractional contribution from aortic versus carotid stretch sensors.

The novelty of this model formulation [compared with that given by Beard et al. (4)] is that it invokes different afferent sensor outputs, associated with the aortic (with firing rate f_{BR1}) and carotid (f_{BR2}) baroreceptors. Here, the simple assumption is made that these two inputs are summed to invoke the combined response. This two-input model is compared with alterative models invoking aortic-only an carotid-only inputs, formulated as follows. The aortic-only model ($g = 1$) accepts input only from the a receptors

$$\frac{\mathrm{d}\phi_{SN}}{\mathrm{d}t} = f_{SN}\left(1 - \phi_{SN}\right) - 2f_1 f_{BR1}\phi_{SN} \quad (1$$

and the carotid-only model ($g = 0$) accepts input only from the carotid receptors

$$\frac{\mathrm{d}\phi_{SN}}{\mathrm{d}t} = f_{SN}\left(1 - \phi_{SN}\right) - 2f_1 f_{BR2}\phi_{SN} \quad (1$$

Finally, heart rate (HR) is assumed proportional to the autonomic tone variable

$$\mathrm{HR} = H_0 + H_1\phi_{SN} \quad (1$$

where $H_0 = 28$ min^{-1} and $H_1 = 156$ min^{-1} are model parameters. The values of H_0 and H_1 are chosen that the maximum achievable HR is 184 min^{-1} and HR = 67 min^{-1} at the average resting baseline ton $\phi_{SN} = 0.25$.

All parameters invoked in the physiologically based model are listed in Table 1. Here, all parameters except f_{SN}, f_1, and g are identified from previous studies and held fixed for the analysis presented belc Parameters f_{SN}, f_1, and g are adjusted on an individual basis to match the measured HR(t) for a given subject.

This model represents a major simplification of previous models, such as the model of Bugenhagen et (6) that accounts for mutually dependent dynamics of parasympathetic and sympathetic efferent firing While lumping sympathetic and parasympathetic effects into a single autonomic tone variable represe simplification, the validity of this simplification in the context of this study is demonstrated by its application. The sympathetic and parasympathetic systems are mutually inhibitory and change in oppc directions in response to changes in arterial pressure (6). Thus, the sympathetic tone variable ϕ_{SN} is interpreted as proportional to the cardiac sympathetic firing rate and inversely proportional to the card vagal parasympathetic firing rate.

Data Fitting and Parameter Estimation

Both the linear filter model and the physiologically based model are fit to data by adjusting parameter minimize the sum of squared difference between model output and measured data. For the linear filter model the objective (error) function was calculated as the sum of squared difference between measure and model-predicted RR interval, determined by *Eq. 2*. The parameters τ and α were constrained to be nonnegative using the MATLAB (The MathWorks, Natick, MA) optimization routine fmincon. For th physiologically based model the objective function was calculated as the sum of the squared differenc between the measured HR and model-predicted value determined by *Eq. 12*.

RESULTS

Baroreflex Response Assessed by Linear Filter Model

Measured arterial pressure, RR interval, and heart rate for three representative subjects are shown in F Results are shown for the subjects for which the linear filter model of *Eq. 2* shows the lowest (*subject* median (*subject 10*), and highest (*subject 3*) mean square error. The responses of *subjects 13* and *10* sl clear increases in heart rate during the Valsalva period and recovery to baseline. The heart rate for *sub 3* follows a less predictable pattern, with relatively little change in heart rate during the measurement. of the linear filter output to data from all 27 subjects are provided in the appendix, Figs. A1–A7.

Summary statistics for the estimated gain α and time constant τ are reported in Table 2. A standard tw sample *t*-test is used to compute *P* values for the probabilities that parameters from male and female groups are drawn from the same statistical distribution. The data reveal no statistically discernable differences in these parameters between the male and female groups. Although the values of τ are low for the female group than for the male group (2.89 ± 2.47 vs. 5.07 ± 3.57 s, means ± SD), the differenc not statistically significant ($P = 0.0759$). The difference in the means may be attributed to the fact that average age of female subjects is ~9 yr less than the average for the male subjects. Trends in the data a explored in more detail in Figs. 4 and 5. Figure 4*A* plots systolic pressure versus age for all study participants, showing no relationship between age and systolic pressure. Nor was there any relationshi between age and diastolic or mean pressure (data not shown). Similarly, there was no significant relationship between age and the estimated gain parameter, plotted in Fig. 4*B*. A plot of estimated tim constant versus age in Fig. 4*C*, on the other hand, reveals a statistically significant increase in estimate with age. Older subjects tend to show a slower response in heart rate to changes in pressure. Similar tr in baroreflex sensitivity (decreasing sensitivity with increasing age) have been observed in previous studies (11, 17).

Data from three outliers, *subjects 6*, *7*, and *17*, are indicated in Fig. 4. *Subject 6* shows an estimated va of τ that is substantially greater than the trend line, with an estimated α that is below the population average. Conversely, *subject 7* shows a relatively rapid response (τ that is substantially lower than the trend line) and high gain. Examining these outliers, we speculate that there may be an inverse relation between α and τ. Indeed, a plot of α/τ (Fig. 4*D*) reveals a significant trend of decreasing α/τ with age. this case the data are fit with a decaying exponential. (The *P* value for the exponential fit is 0.019 compared with $P = 0.069$ for a linear fit.) *Subject 7* is the greatest outlier from the observed trend in α versus age, with the second highest value of α/τ despite being one of the older subjects (age = 59 yr).

Figure 5*A* plots relationships between the baroreflex response time τ and the resting systolic pressure. the data reveal a statistically significant relationship between systolic pressure and τ ($P < 0.01$). The strength of this relationship is surprising because a diagnosis of hypertension was an exclusion criteric for the study. The positive correlations between age and τ and between systolic pressure and τ, along v a lack of correlation between age and systolic pressure, indicate that systolic pressure and age are independent predictors of τ. Indeed, combining age and systolic pressure in a multiple regression (Fig shows that taken together, age and systolic pressure predict τ with a correlation coefficient of 0.627. Furthermore, we notice that the correlation between τ and systolic pressure (Fig. 5*A*) is less strong for largest values of τ. Excluding the seven individuals with estimated τ > 5 s, the correlation and *P* value the linear regression become $r = 0.755$ and $P = 1.2 \times 10^{-4}$, respectively.

Prior studies have shown that baroreflex sensitivity diminishes with increasing age and increasing blo pressure (5, 10, 16, 17). However, these studies have reported baroreflex sensitivity in terms of chang heart rate interval per unit change in pressure, measured over a defined time interval. Thus, they do nc separate out effects of the speed of response versus overall gain. Our simple linear analysis, which separates the gain and the speed of the response, reveals no significant relationships between the filter α and age or between α and blood pressure. These findings indicate that the response time, rather than gain, is the more important indicator of changes in baroreflex function that occur with age and change cardiovascular health.

Baroreflex Response Assessed by Physiologically Based Model

The physiologically based model uses the measured expiratory pressure (P_{th}) as a model input via *Eq.* addition to the measured arterial pressure, to predict heart rate (HR). As an illustrative example, arteri pressure, predicted aortic and carotid diameters, and heart rate are shown in Fig. 6 for *subject 4*. The measured expiratory pressure for this subject is shown in Fig. 1. The simulated diameters (Fig. 6*B*) sh that during the Valsalva period, the influence of the compressive pressure results in lower relative diameters for the aorta compared with the carotids. When the Valsalva is released, the carotid strain is predicted to drop sharply as the arterial pressure drops sharply. However, while the carotid strain is dropping (around $t = 32$ s), the aortic strain is predicted to be increasing because of the release of the compressive pressure associated with the Valsalva.

The consequences of different strain signals originating from the aortic versus carotid strain sensors ar explored in Fig. 6*C*. The predicted heart rate associated with the aortic-only model ($g = 1$) does not ca the peak in heart rate that follows the release of the Valsalva, because the aortic strain does not experie the rapid drop predicted for the carotid. Although the carotid-only model ($g = 0$) is able to capture the Valsalva heart rate peak, the carotid-only model predicts an initial drop in heart rate that is too large ar too late in the early phase 2 response. Only the combined model (Fig. 6*D*, $g = 0.5$) is able to effectivel capture all features of the observed heart rate response.

The physiologically based model was applied to the same data set analyzed using the linear filter mod by adjusting the three parameters f_{SN}, f_1, and g on an individual basis to match the measured HR(t) fo each subject. Model fits for all 27 subjects are shown in Figs. A8–A14 of the appendix. Statistics for model parameters are summarized in Table 2. As for the simple filter model, we find no significant differences between male and female groups (2-sample *t*-test).

Figure 7 illustrates a variety of trends observed in the parameter estimates for the physiologically base model. Figure 7*A* shows that there is a strong correlation between the rates f_{SN} and f_1. This is not surprising since these parameters, invoked in *Eq. 9*, represent opposing influences on autonomic tone. the system to attain a resting heart rate in a physiologically reasonable range, these rates increase and decrease in approximate proportion. Since these parameters govern the autonomic response rate, we expected to see a relationship between their values and age, similar to the relationship between age an time constant τ from the linear filter model. Indeed, as illustrated in Fig. 7, *B* and *C*, the estimated rate and f_1 tend to decrease with age. Figure 7*D* shows that $1/f_{SN}$ from the physiologically based model is strongly correlated with τ estimated from the linear filter model. This correlation is expected because τ and $1/f_{SN}$ represent rate constants governing the rate of response of the respective models to changes pressure.

Although the plots in Fig. 7 reveal significant trends in the rates f_{SN} and f_1 that govern how the centra nervous system processes and responds to afferent inputs, these relationships should not be interpreted necessarily reflecting changes to central autonomic function occurring with age. Since independent da the mechanical properties of the large arteries in the individual subjects were not available, the model using the physiologically based model employed fixed parameters (μ, k', and D', Table 1) to represent mechanical properties of the aorta and carotid sinus. Furthermore, since independent data on afferent were not obtained, parameters governing how afferent firing responds to changes in strain (τ_s, δ_o, a, b f_o) were held fixed. Thus, this model analysis is not able to detect any potential differences in afferent function that may underlie the individual variability in the baroreflex response observed in this study. differences and trends in estimated values of f_{SN}, f_1, and g may more accurately reflect differences in arterial mechanical properties or afferent strain sensor properties. For example, a relatively slow respo time, reflected in a large value of τ for the linear filter model, and slow rate constants (f_{SN} and f_1) for physiologically based model, may mechanistically arise from relatively high values of effective stiffne and/or viscosity of the walls of the large arteries associated with the strain sensors. In other words, in present analysis, variabilities in the central physiologically based model parameters f_{SN} and f_1, or equivalently the filter model time constant τ, are used as proxies to represent potential variability at ar stage of the baroreflex arc: from arterial wall mechanics, to afferent firing dynamics, to central autono function. Differences in estimated values of these parameters reflect differences in overall responsiver of the baroreflex system to changes in arterial pressure but do not necessarily pinpoint the underlying sources of variability.

DISCUSSION

We have introduced two methods to assess baroreflex function from data on arterial pressures, heart ra and expiratory pressure occurring with the Valsalva maneuver in human subjects. The two methods, o based on a phenomenological linear filter model of the baroreflex arc and one based on a physiologica based model, provide similar insights into relationships between the responsiveness of the baroreflex system and age and the responsiveness of the system and systolic arterial pressures.

Linear Filter Model

The simple linear filter model for the heart rate response to changes in pressure of *Eq. 1* distinguishes parameters representing response time (τ) from gain (α). Previous analyses conflate these components

a baroreflex sensitivity parameter. Our analysis predicts that the response rate (captured by τ) reflects changes to the baroreflex arc that occur with aging, whereas the gain parameter (α) shows no clear tre with age. Difference in response time may be related to differences in viscoelastic properties of vessel containing the stretch receptors or may be related to difference in central autonomic function.

Findings illustrated in Fig. 5 indicating that τ is associated with resting systolic pressure in normal sub point to the potential utility of this parameter as a predictor of cardiovascular risk. Future larger-scale studies are needed to determine how baroreflex response time [and other metrics derived from this ana such as gain (α)] may or may not be useful in assessing cardiovascular fitness and risk. Based on the relationship observed in Fig. 5*A*, we speculate that this analysis may be able to reveal the degree to wh baroreflex dysfunction contributes to development of hypertension.

Physiologically Based Model

Although the physiologically based model is designed to capture baroreflex function with more mechanistic meaning than the simple linear filter model, it should not be interpreted as providing a quantitatively better match to the data than the simpler model. The physiologically based model does tend to fit the Valsalva data any better (or worse) than the simpler model. Yet it does potentially reveal more insight into physiological function than the linear filter. For example, the physiologically based model analysis was used to illustrate that different signals from carotid versus aorta are important in governing the response to Valsalva. Previous studies have speculated that carotid versus aortic afferen respond in opposite ways during the initial phase of the Valsalva response (31). Our analysis provides quantitative estimation of how arterial strain in the carotid sinus and aortic arch tends to change in opposite directions not only in the initial phase of the Valsalva but also when the Valsalva is released. the initial phase, the increase in arterial pressure causes an overall distension in carotid diameters that not seen in the aortic arch due to external compression from the elevated thoracic pressure. When the Valsalva is released, the drop in thoracic pressure allows the aortic diameter averaged over the cardiac cycle to increase, even as the mean arterial pressure temporarily drops. For the first few seconds follo release of the Valsalva only the carotid baroreceptors are able to sense a decrease in average pressure/strain, and thus the carotid baroreceptors are responsible for the transient increase in heart rat that occurs following the release of the Valsalva.

The major limitation of the physiologically based model analysis is that the model invokes a number parameters that cannot be estimated from the data obtained in this study. Specifically, parameters representing arterial mechanical properties (μ, k', and D') are set to values obtained from analysis of a healthy individual. Parameters associated with the afferent response to strain rate (τ_s, δ_o, a, b, and f_0) set to values obtained from studies on large animals (4). By adjusting parameters (f_{SN}, f_1, and g) that govern the response of autonomic tone to fit data from individuals, our analysis is not able to capture variability in responses that may be governed by differences in mechanical properties and/or afferent sensor function. In other words, our analysis lumps likely sources of variability into the parameters representing effector response. Given the large number of parameters (fixed and adjusted), there are li to be multiple combinations of parameters that could be assigned as adjustable to fit the data. Evaluati which combinations could be used and which could not would be a computationally expensive proces is beyond the scope of the present study. For example, although differences in arterial mechanical properties may underlie differences in baroreflex responses (13, 22, 28), the present analysis is not ab

detect this or other potential mechanisms underlying the variability in the population.

Similarly, the linear filter model lumps a series of physiological functions (arterial strain, afferent firir central processing, and efferent output) into a phenomenological response captured by a simple linear filter. The linear filter model has the advantage that its relatively few parameters may be identified fro the time course data obtained here. On the other hand, the greater mechanistic fidelity of the physiologically based model provides a scaffold on which different sources of variability can be accou for, given independent data on the subsystems from which the physiological model is constructed. For example, independent measurements of arterial stiffness (1) could be incorporated into the individual parameterization of the physiologically based model to more effectively capture the physiological bas individual variability in the baroreflex response.

Although the model is able to at least qualitatively represent the observed response for most subjects, several of the cases the model fails to capture the observed trends. Many subjects show a characteristi oscillation in heart rate during the pre-Valsalva period (cf. *subjects 2*, *8*, *12*, and *19*). These oscillation likely associated with respiration, a phenomenon not accounted for in the model. Furthermore, many subjects show a transient peak in heart rate immediately preceding the Valsalva (cf. Fig. 6). This spike heart rate is associated with a rapid inhalation taken in preparation for the Valsalva. Again, this phenomenon is not accounted for in our model. Moreover, analysis for several subjects reveals an inab to effectively capture the heart rate response during and after the Valsalva period. For example, the physiologically based model largely fails to represent the heart rate dynamics of *subject 1*, for which t arterial pressure did not show the expected characteristic pattern illustrated in Fig. 6. Specifically, for subject, mean pressure increases immediately at the onset of the Valsalva maneuver as it does for mos subjects. However, although the heart rate gradually increases during the Valsalva period, neither the p pressure nor the mean pressure drop substantially, resulting in an inability of the model to capture the response. Although the linear filter model for this subject does a better job of matching the data, it stil fails to match the full extent of increase in heart rate that occurred during the Valsalva.

Subjects 7 and *25* are additional examples for whom neither the linear filter nor the physiologically ba model effectively captures the data. Similar to the pressure recorded for *subject 1*, the pressures do no drop substantially during the Valsalva period for either of these subjects. (Compare the pressures in Fig. A14 for *subjects 25* and *26*.) The fit to the data for *subject 7* using the physiological model (Fig. A yields values of f_{SN} and f_1 that are outliers in the plots in Fig. 4 and result in rapid oscillations in the model-predicted HR(t).

Limitations of Study

In addition to the simplifying assumptions invoked in the model analyses discussed in METHODS, the conclusions of this study are influenced and limited by the relatively small cohort of subjects and exclusion criteria used to define that cohort. The finding that age and systolic blood pressure are uncorrelated, for example, should not be taken as reflecting the broader population because hypertensi subjects were excluded from the study. Furthermore, given the small size of the study, it is not possibl control for other hidden correlates of arterial pressure and autonomic function, such as exercise trainir race, body mass index, etc. Since this study was (by design) biased against potentially observing a relationship between age and arterial pressure, it is unknown how the observed trends in autonomic

function vary in the broader population. We hypothesize that suppressed autonomic control of heart ra a contributing factor to the etiology of primary hypertension, rather than only a compensatory sequela That we observe relationships between reduced autonomic responsiveness and age and between reduc autonomic responsiveness and systolic pressure is consistent with the specific hypothesis that suppres of autonomic reflexes occurs independently of and can precede hypertension. Further testing of these hypotheses will require substantially larger-scale studies.

Major Findings

The major findings of the study can be summarized as follows.

1. The effective response time of the baroreflex arc tends to increase with age in healthy subjects (Fig. 4*C*). Equivalently, the effective response rate decreases with age.
2. The response time/response rate is a predictor of systolic pressure (Fig. 5*A*) based on observation from a group of 27 healthy volunteers.
3. Analysis of the Valsalva response using a physiologically based model (Fig. 6) reveals that differ afferent inputs from the carotid sinus and the aortic arch baroreceptors govern different parts of th heart rate response.

GRANTS

This work was supported by NIH National Heart, Lung, and Blood Institute Grant HL-139813 to D.A Beard.

DISCLOSURES

No conflicts of interest, financial or otherwise, are declared by the authors.

AUTHOR CONTRIBUTIONS

S.A.K., B.E.C., S.L.H., R.D.B., and D.A.B. conceived and designed research; S.A.K. performed experiments; S.A.K. and D.A.B. analyzed data; S.A.K. and D.A.B. interpreted results of experiments; S.A.K. and D.A.B. prepared figures; S.A.K. and D.A.B. drafted manuscript; S.A.K., B.E.C., S.L.H., R.D.B., and D.A.B. edited and revised manuscript; S.A.K., B.E.C., S.L.H., R.D.B., and D.A.B. appro final version of manuscript.

ENDNOTE

At the request of the authors, readers are herein alerted to the fact that additional materials related to t manuscript may be found at PhysioNet.org, which at the time of publication they indicate is: https://physionet.org/physiobank/database/rvmh1/. These materials are not a part of this manuscript ar have not undergone peer review by the American Physiological Society (APS). APS and the journal editors take no responsibility for these materials, for the Web site address, or for any links to or from i

APPENDIX

This appendix contains Figs. A1–A14, plotting the fits of the linear filter model and the physiological

based model to the data from the 27 subjects analyzed in this study. Data collected from all subjects ar freely available on PhysioNet.org (9a; https://physionet.org/physiobank/database/rvmh1/).

Fig. A1.

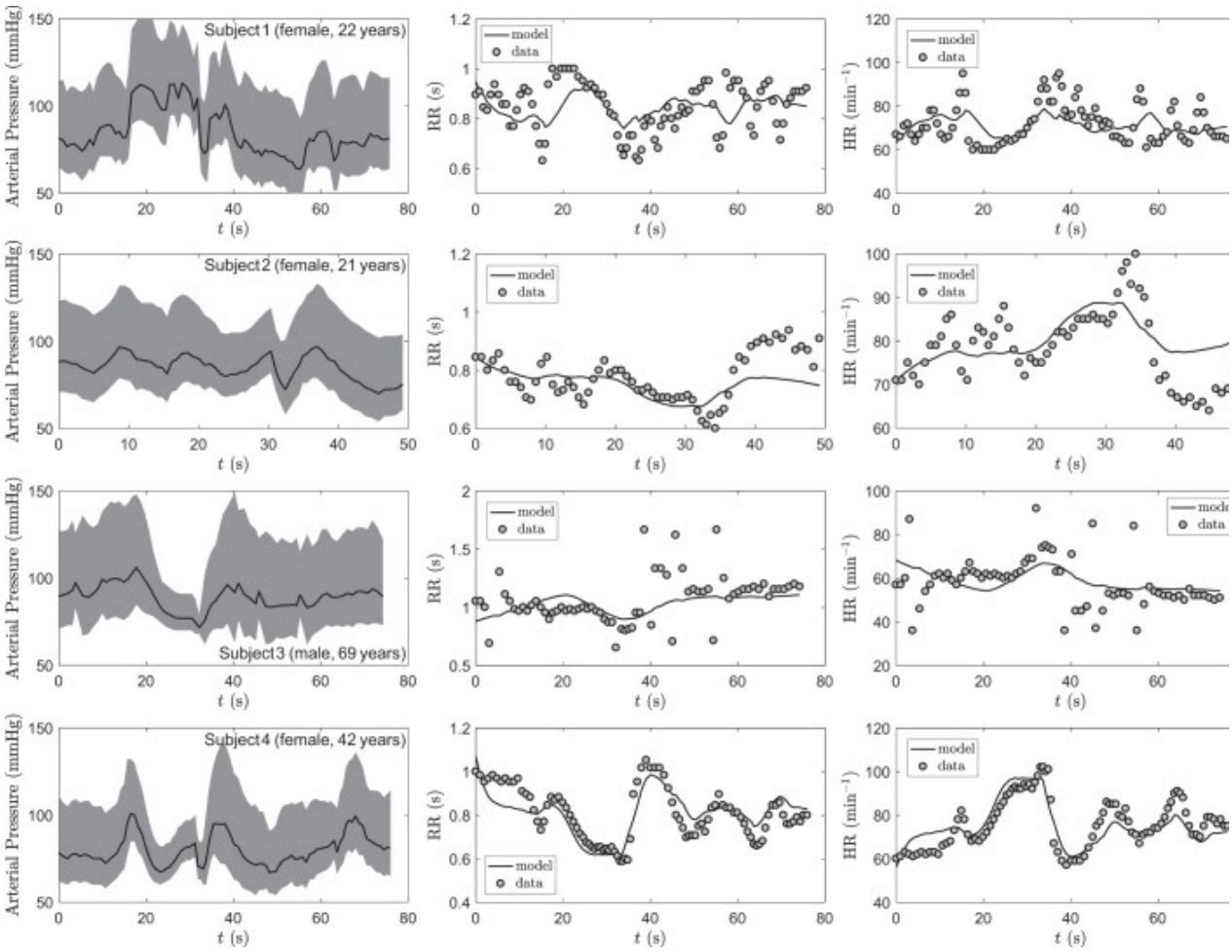

Arterial pressures, R-R intervals, heart rate responses to Valsalva, and linear filter model fits for *subjects 1–4*. Panels at *left* illustrate measured arterial pressure, panels in *middle* illustrate measured R-R interval (RR) and fits of *Eq. 2*, and panels at *right* show the measured and model-fit heart rate (HR).

Fig. A2.

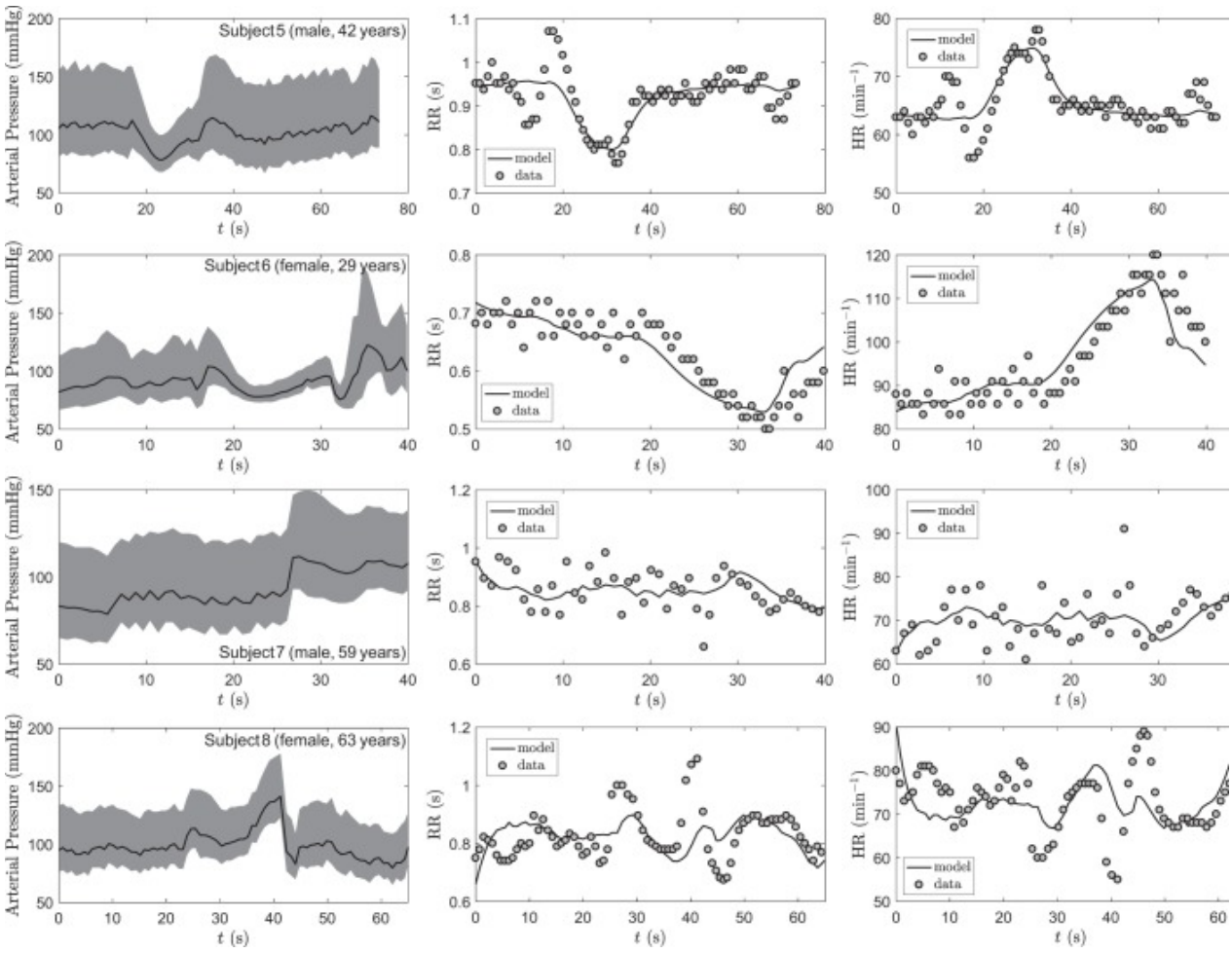

Arterial pressures, R-R intervals, heart rate responses to Valsalva, and linear filter model fits for *subjects 5–8*. Panels at *left* illustrate measured arterial pressure, panels in *middle* illustrate measured R-R interval (RR) and fits of *Eq. 2*, and panels at *right* show the measured and model-fit heart rate (HR).

Fig. A3.

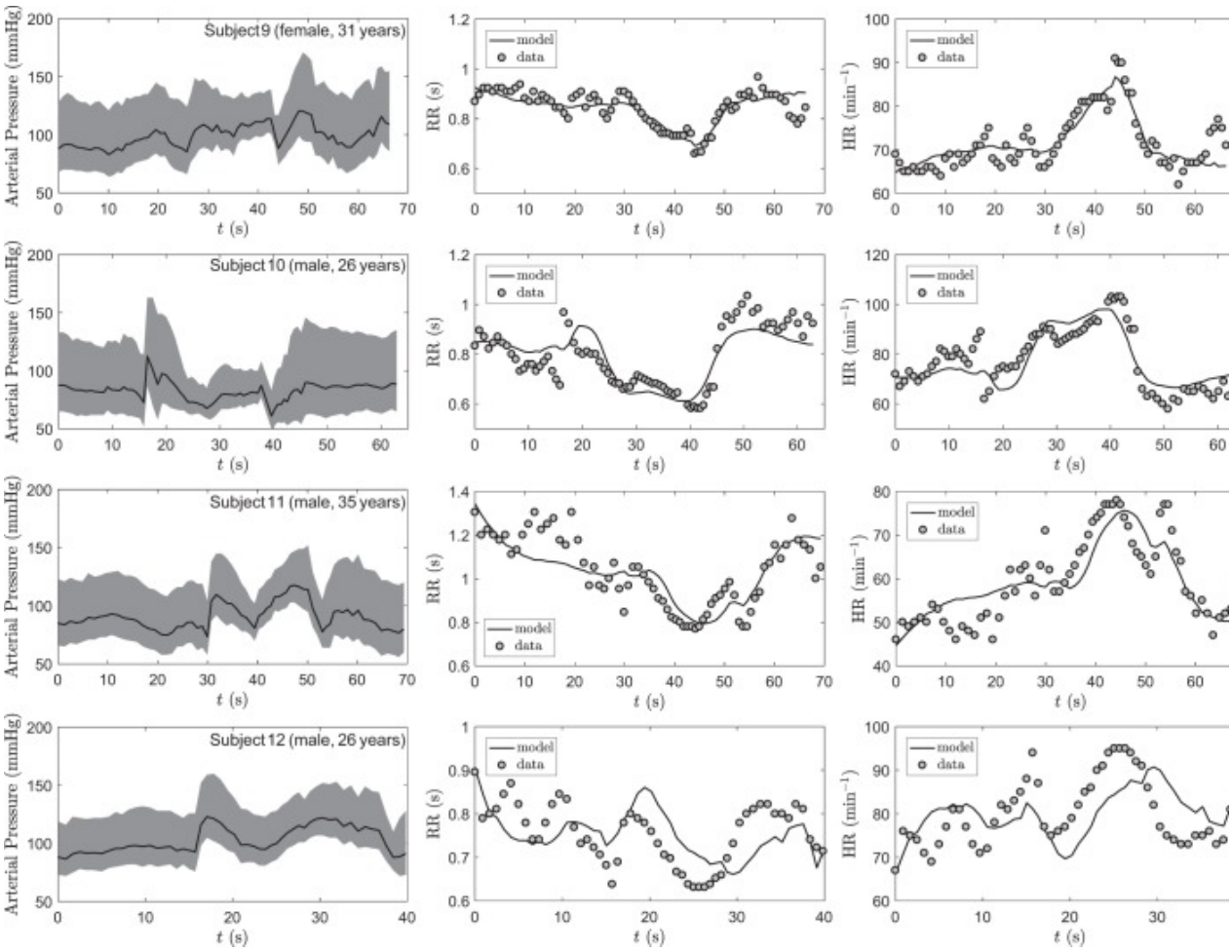

Arterial pressures, R-R intervals, heart rate responses to Valsalva, and linear filter model fits for *subjects 9–12*. Panels at *left* illustrate measured arterial pressure, panels in *middle* illustrate measured R-R interval (RR) and fits of *Eq. 2*, and panels at *right* show the measured and model-fit heart rate (HR).

Fig. A4.

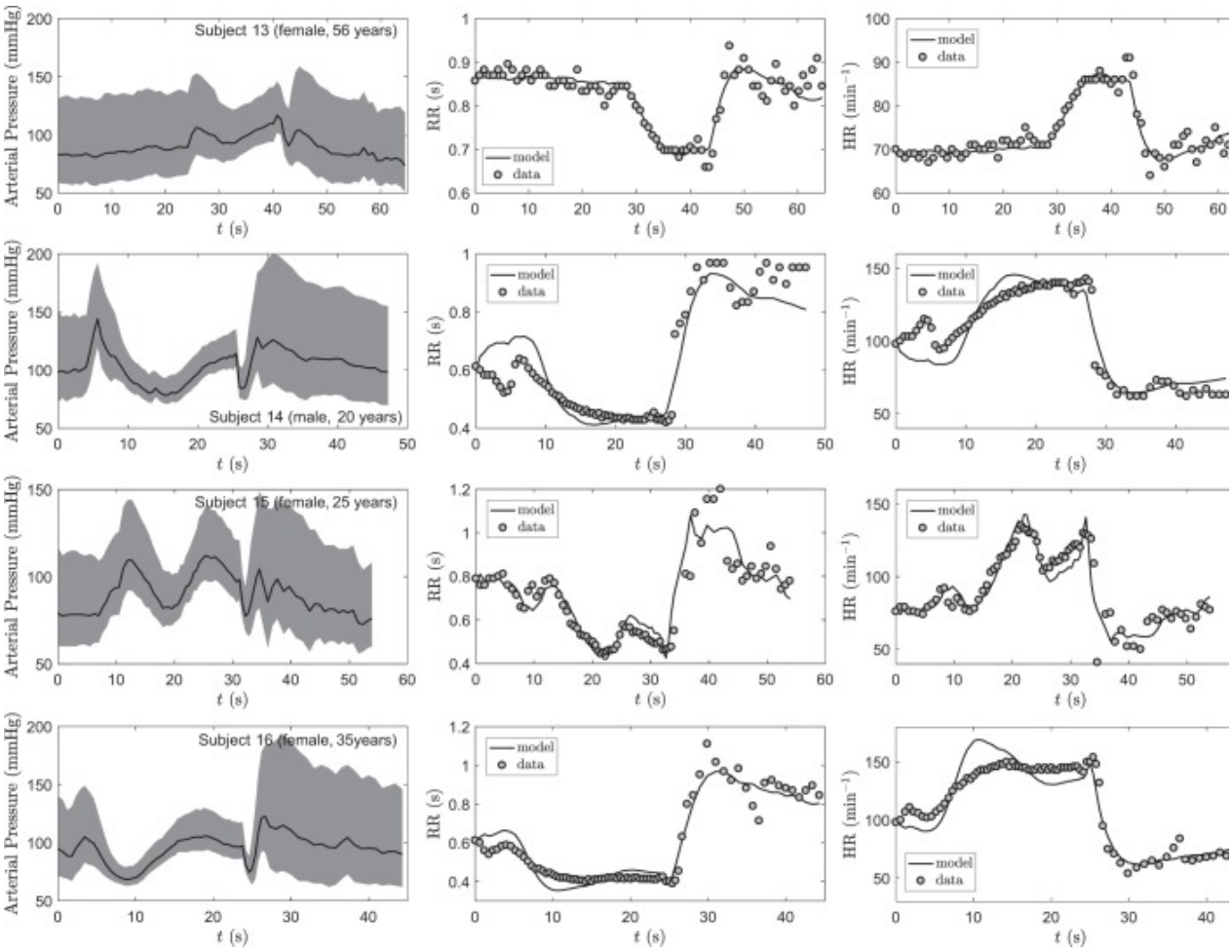

Arterial pressures, R-R intervals, heart rate responses to Valsalva, and linear filter model fits for *subjects 13–16*. Panels at *left* illustrate measured arterial pressure, panels in *middle* illustrate measured R-R interval (RR) and fits of *Eq. 2*, and panels at *right* show the measured and model-fit heart rate (HR).

Fig. A5.

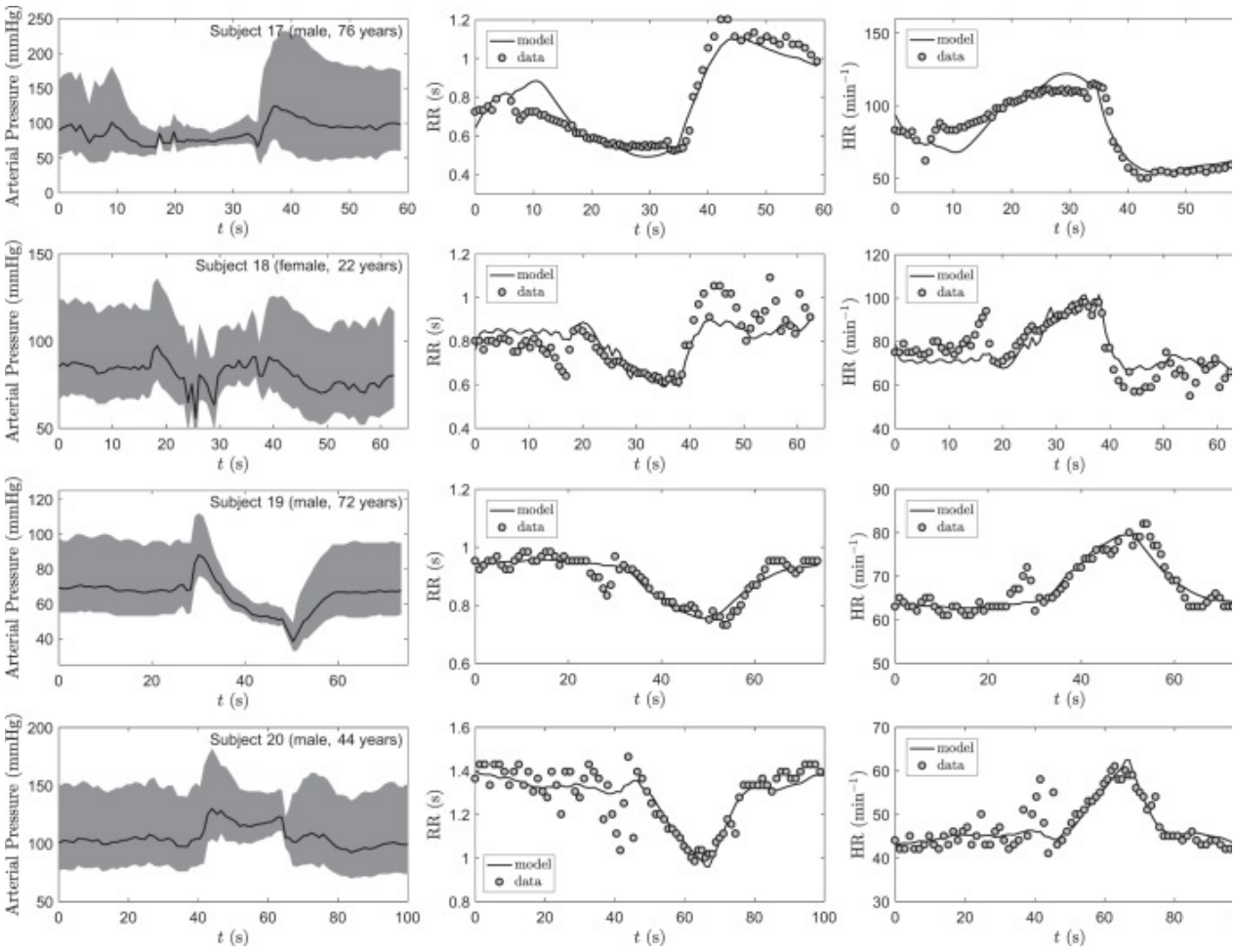

Arterial pressures, R-R intervals, heart rate responses to Valsalva, and linear filter model fits for *subjects 17–20*. Panels at *left* illustrate measured arterial pressure; panels in *middle* illustrate measured R-R interval (RR) and fits of *Eq. 2*, and panels at *right* show the measured and model-fit heart rate (HR).

Fig. A6.

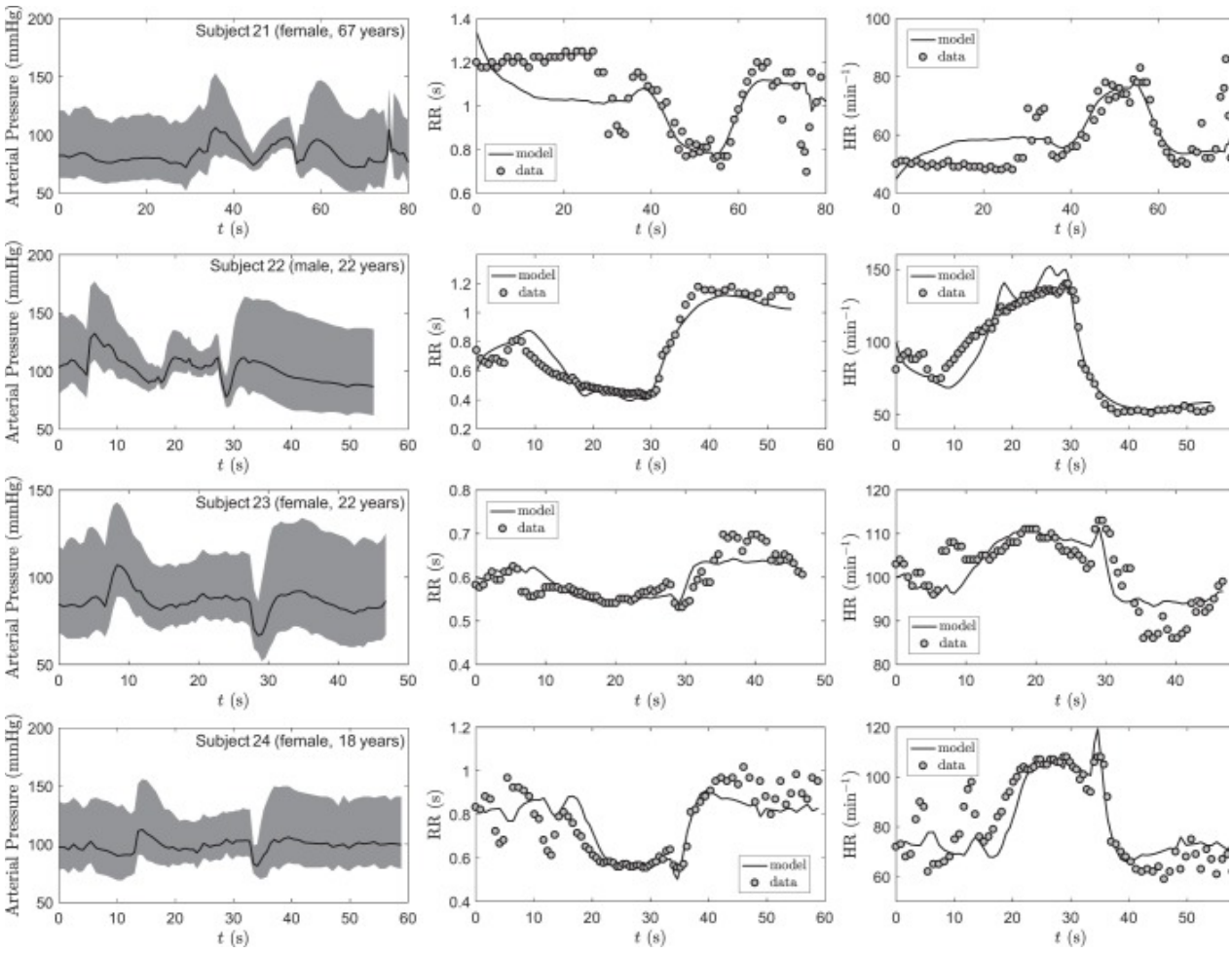

Arterial pressures, R-R intervals, heart rate responses to Valsalva, and linear filter model fits for *subjects 21–24*. Panels at *left* illustrate measured arterial pressure, panels in *middle* illustrate measured R-R interval (RR) and fits of *Eq. 2*, and panels at *right* show the measured and model-fit heart rate (HR).

Fig. A7.

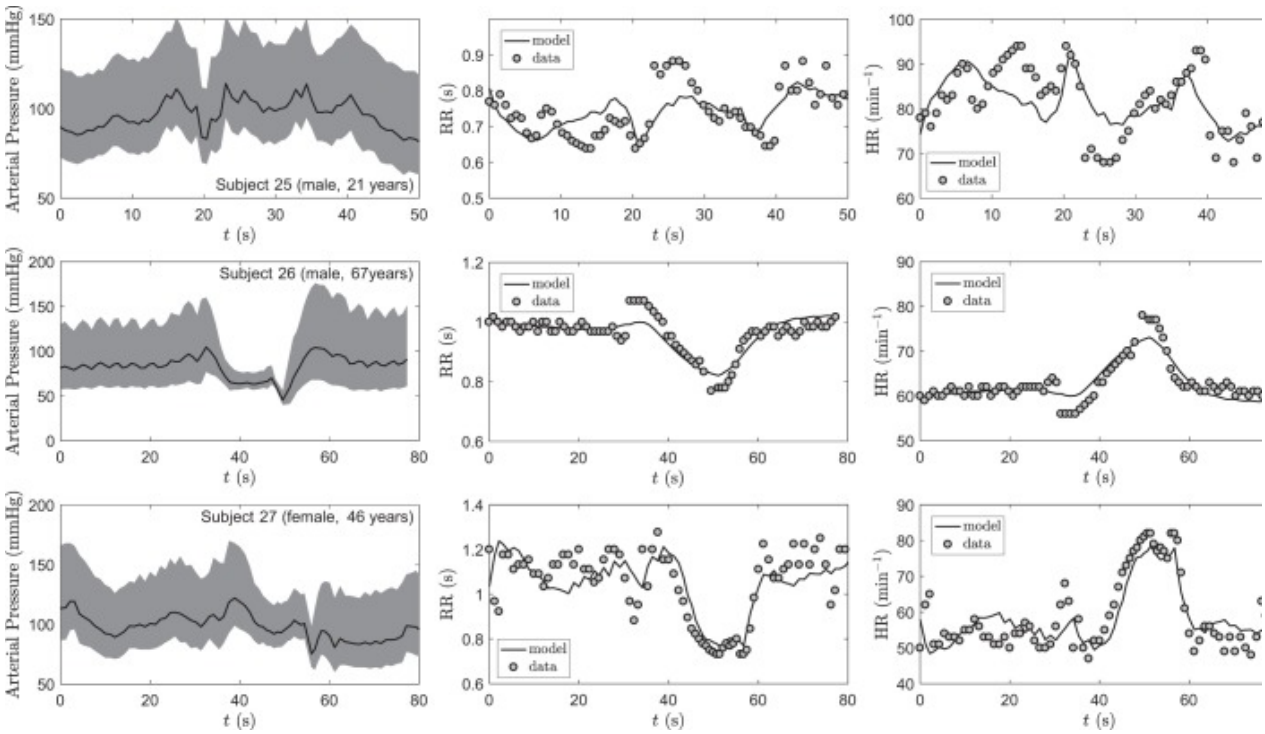

Arterial pressures, R-R intervals, heart rate responses to Valsalva, and linear filter model fits for *subjects 25–27*. Panels at *left* illustrate measured arterial pressure, panels in *middle* illustrate measured R-R interval (RR) and fits of *Eq. 2*, and panels at *right* show the measured and model-fit heart rate (HR).

Fig. A8.

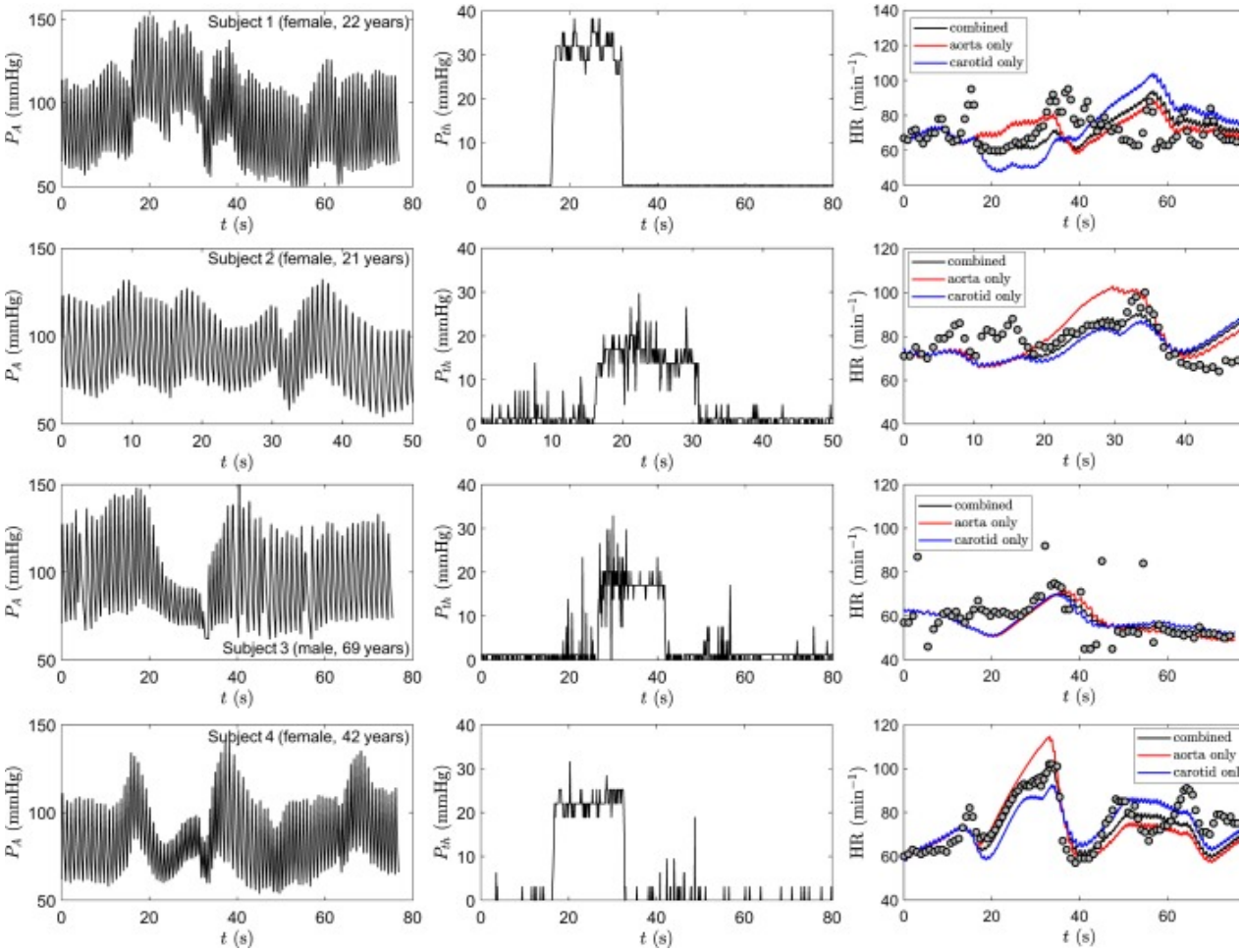

Arterial and thoracic pressures, heart rate responses to Valsalva, and physiologically based model fits for *subject 1–4*. Panels at *left* illustrate measured arterial pressure (P_A), panels in *middle* illustrate measured thoracic pressu (P_{th}), and panels at *right* show the measured and model-fit heart rate (HR).

Fig. A9.

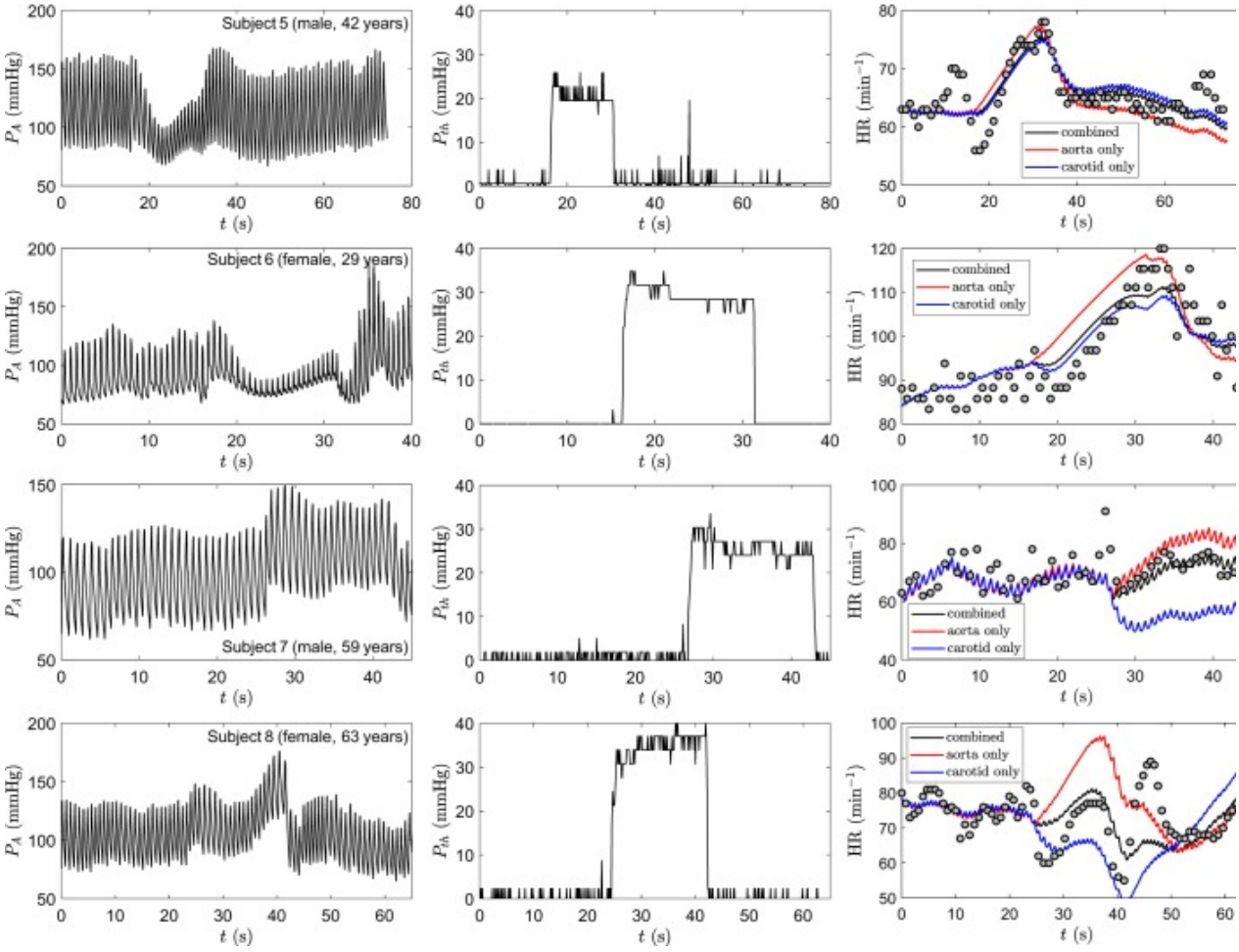

Arterial and thoracic pressures, heart rate responses to Valsalva, and physiologically based model fits for *subject 5–8*. Panels at *left* illustrate measured arterial pressure (P_A), panels in *middle* illustrate measured thoracic pressu (P_{th}), and panels at *right* show the measured and model-fit heart rate (HR).

Fig. A10.

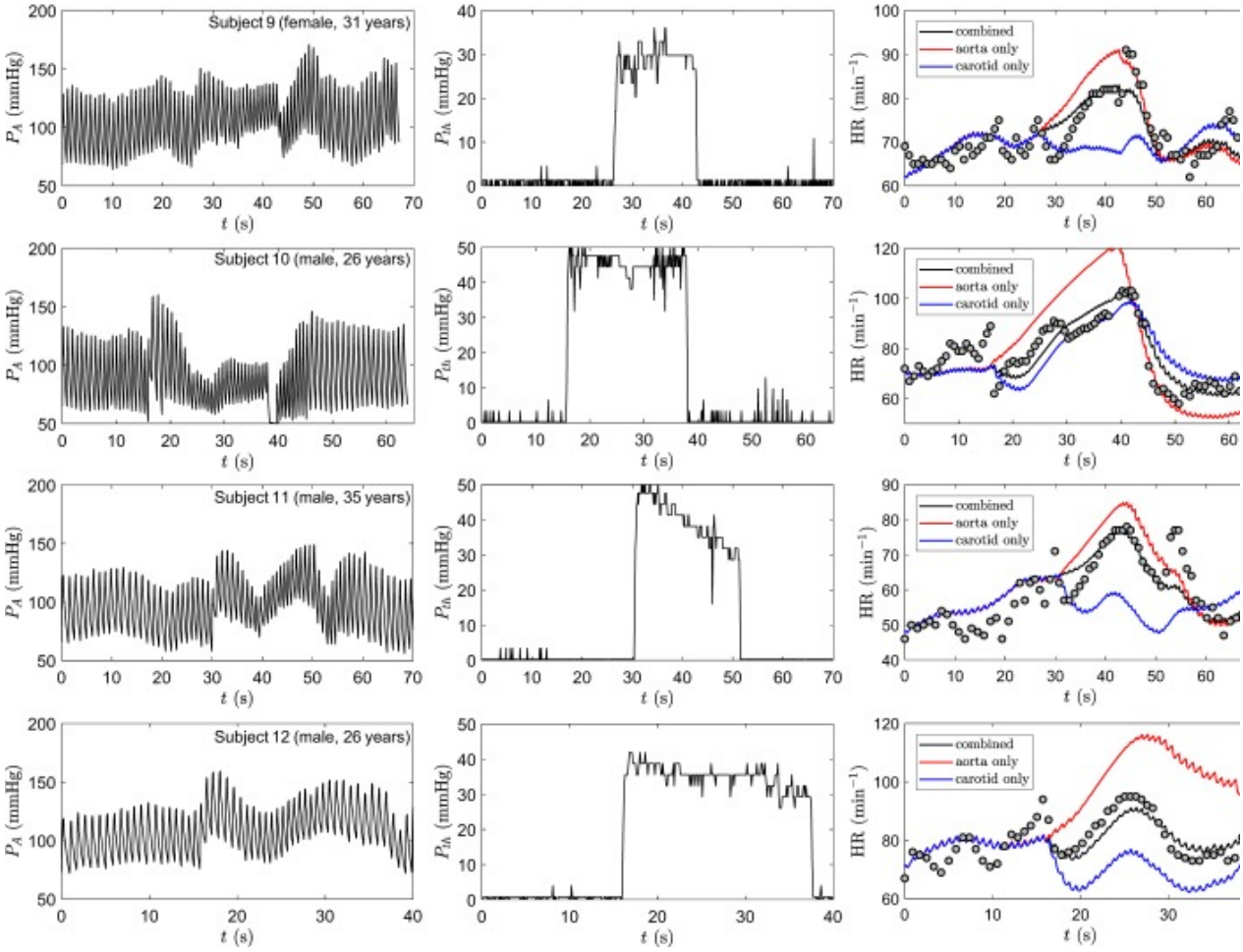

Arterial and thoracic pressures, heart rate responses to Valsalva, and physiologically based model fits for *subject 9–12*. Panels at *left* illustrate measured arterial pressure (P_A), panels in *middle* illustrate measured thoracic pressure (P_{th}), and panels at *right* show the measured and model-fit heart rate (HR).

Fig. A11.

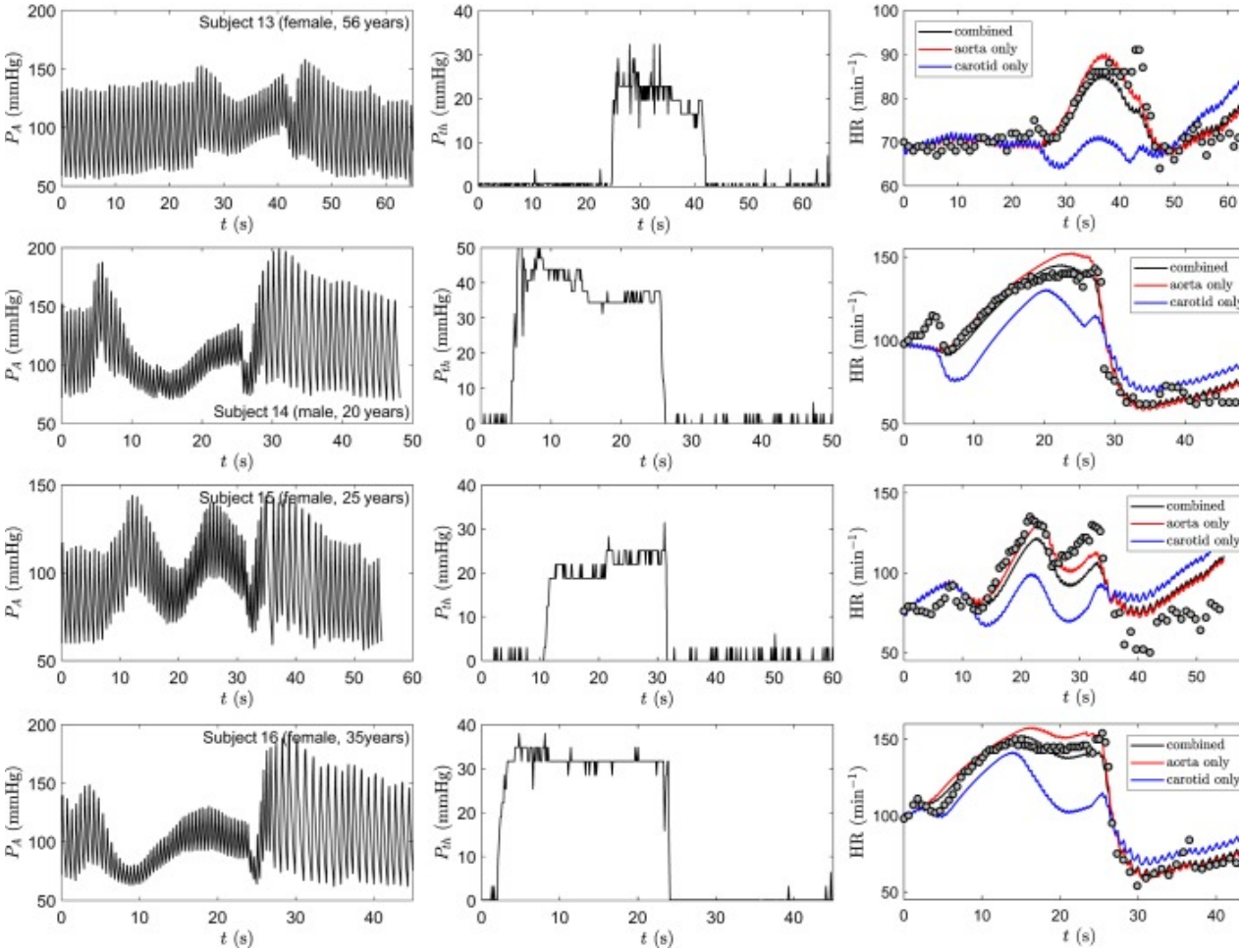

Arterial and thoracic pressures, heart rate responses to Valsalva, and physiologically based model fits for *subject 13–16*. Panels at *left* illustrate measured arterial pressure (P_A), panels in *middle* illustrate measured thoracic pressure (P_{th}), and panels at *right* show the measured and model-fit heart rate (HR).

Fig. A12.

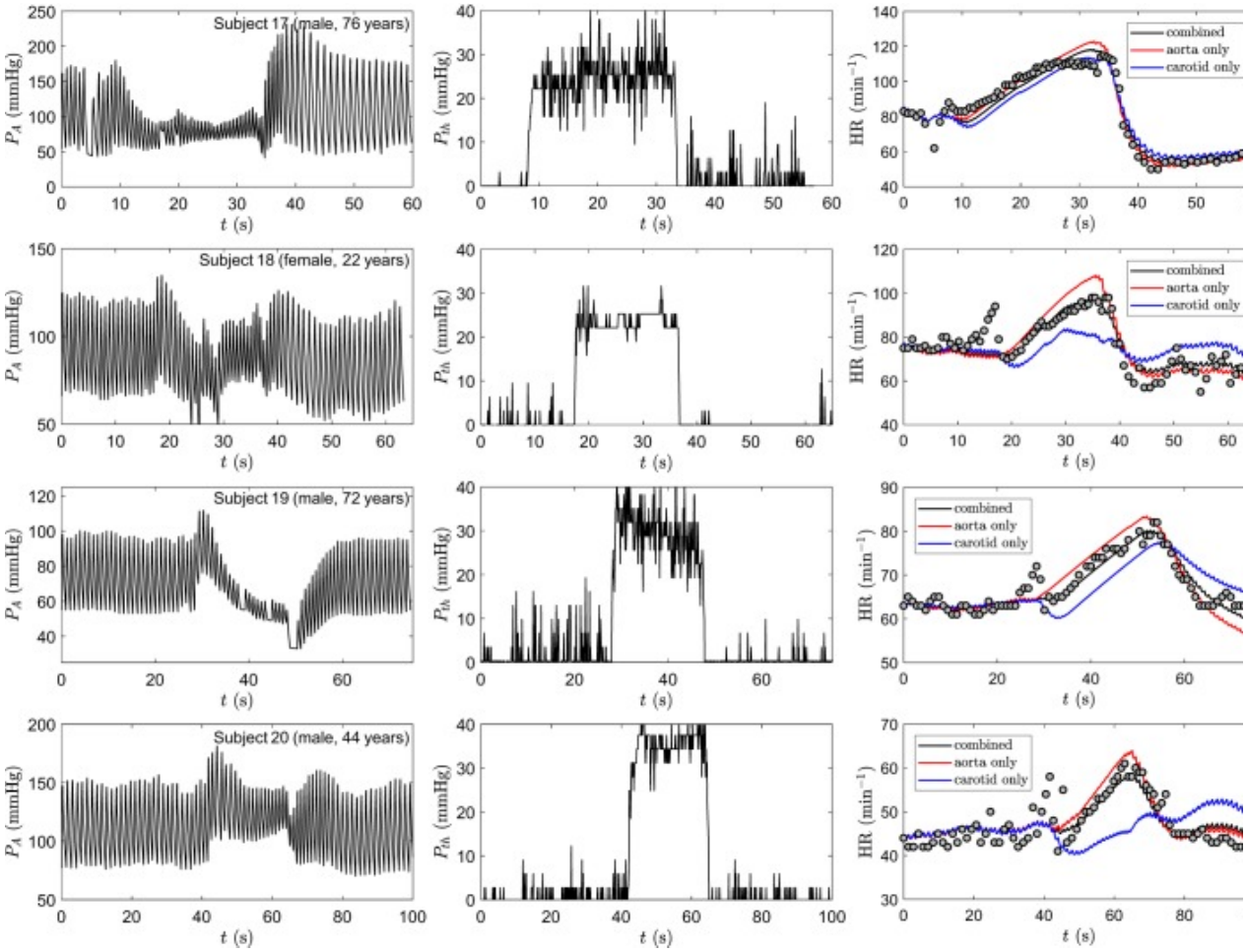

Arterial and thoracic pressures, heart rate responses to Valsalva, and physiologically based model fits for *subject 17–20*. Panels at *left* illustrate measured arterial pressure (P_A), panels in *middle* illustrate measured thoracic pressure (P_{th}), and panels at *right* show the measured and model-fit heart rate (HR).

Fig. A13.

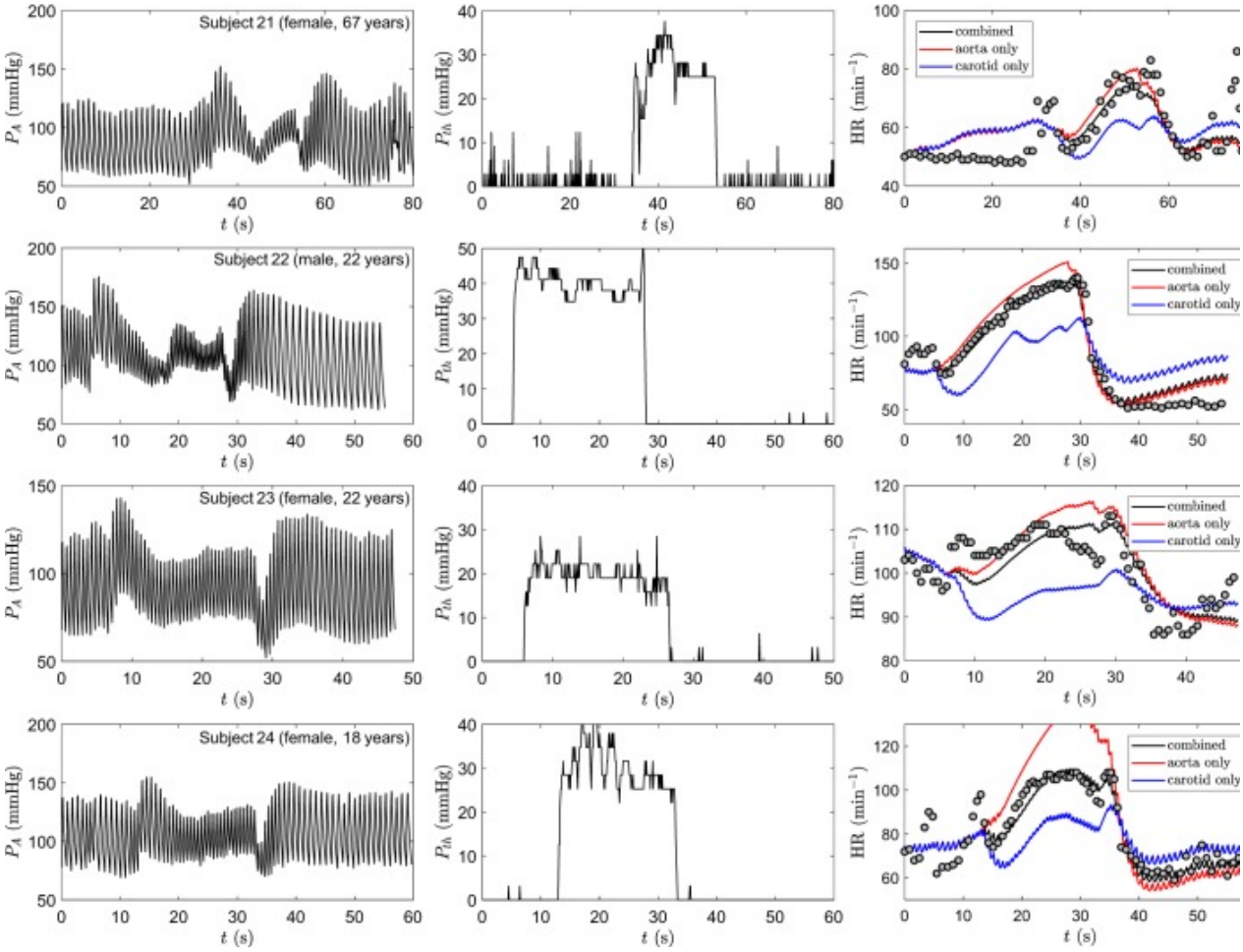

Arterial and thoracic pressures, heart rate responses to Valsalva, and physiologically based model fits for *subject 21–24*. Panels at *left* illustrate measured arterial pressure (P_A), panels in *middle* illustrate measured thoracic pressure (P_{th}), and panels at *right* show the measured and model-fit heart rate (HR).

Fig. A14.

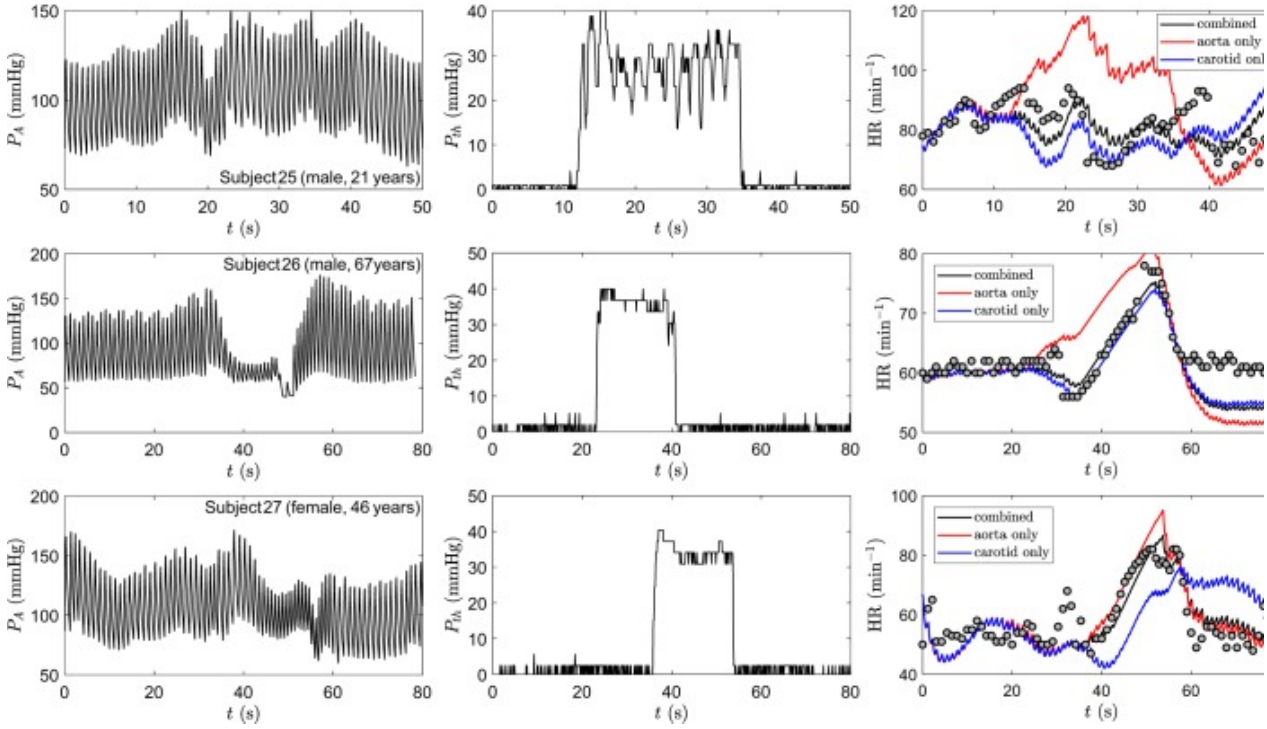

Arterial and thoracic pressures, heart rate responses to Valsalva, and physiologically based model fits for *subject 25–27*. Panels at *left* illustrate measured arterial pressure (P_A), panels in *middle* illustrate measured thoracic pressure (P_{th}), and panels at *right* show the measured and model-fit heart rate (HR).

REFERENCES

1. Aquaro GD, Cagnolo A, Tiwari KK, Todiere G, Bevilacqua S, Di Bella G, Ait-Ali L, Festa P, Glaub M, Lombardi M. Age-dependent changes in elastic properties of thoracic aorta evaluated by magnetic resonance in normal subjects. *Interact Cardiovasc Thorac Surg* 17: 674–679, 2013. doi:10.1093/icvts/ivt261. [PMCID: PMC3781791] [PubMed: 23760356] [CrossRef: 10.1093/icvts/ivt261]

2. Beard DA. Tautology vs. physiology in the etiology of hypertension. *Physiology (Bethesda)* 28: 270–271, 2013. doi:10.1152/physiol.00038.2013. [PMCID: PMC3768096] [PubMed: 23997184] [CrossRef: 10.1152/physiol.00038.2013]

3. Beard DA, Mescam M. Mechanisms of pressure-diuresis and pressure-natriuresis in Dahl salt-resist and Dahl salt-sensitive rats. *BMC Physiol* 12: 6, 2012. doi:10.1186/1472-6793-12-6. [PMCID: PMC3536597] [PubMed: 22583378] [CrossRef: 10.1186/1472-6793-12-6]

4. Beard DA, Pettersen KH, Carlson BE, Omholt SW, Bugenhagen SM. A computational analysis of t long-term regulation of arterial pressure. *F1000 Res* 2: 208, 2013. doi:10.12688/f1000research.2-208. [PMCID: PMC3886803] [PubMed: 24555102] [CrossRef: 10.12688/f1000research.2-208.v1]

5. Bristow JD, Honour AJ, Pickering GW, Sleight P, Smyth HS. Diminished baroreflex sensitivity in h blood pressure. *Circulation* 39: 48–54, 1969. doi:10.1161/01.CIR.39.1.48. [PubMed: 4302539] [Cross 10.1161/01.CIR.39.1.48]

6. Bugenhagen SM, Cowley AW Jr, Beard DA. Identifying physiological origins of baroreflex dysfun in salt-sensitive hypertension in the Dahl SS rat. *Physiol Genomics* 42: 23–41, 2010. doi:10.1152/physiolgenomics.00027.2010. [PMCID: PMC2888563] [PubMed: 20354102] [CrossRef: 10.1152/physiolgenomics.00027.2010]

7. Castiglioni P, Di Rienzo M, Parati G. How should the baroreflex sensitivity on the heart be estimate *Electrocardiol* 44: 391–392, 2011. doi:10.1016/j.jelectrocard.2011.01.006. [PubMed: 21353238] [CrossRef: 10.1016/j.jelectrocard.2011.01.006]

8. Ebert TJ, Cowley AW Jr. Baroreflex modulation of sympathetic outflow during physiological incre of vasopressin in humans. *Am J Physiol Heart Circ Physiol* 262: H1372–H1378, 1992. doi:10.1152/ajpheart.1992.262.5.H1372. [PubMed: 1590441] [CrossRef: 10.1152/ajpheart.1992.262.5.H1372]

9. Eckberg DL, Sleight P. *Human Baroreflexes in Health and Disease*. Oxford, UK: Clarendon, 1992.

9a. Goldberger AL, Amaral LA, Glass L, Hausdorff JM, Ivanov PC, Mark RG, Mietus JE, Moody GE Peng CK, Stanley HE. PhysioBank, PhysioToolkit, and PhysioNet: components of a new research res for complex physiologic signals. *Circulation* 101: e215–e220, 2000. doi:10.1161/01.CIR.101.23.e215 [PubMed: 10851218] [CrossRef: 10.1161/01.CIR.101.23.e215]

10. Goldstein DS. Arterial baroreflex sensitivity, plasma catecholamines, and pressor responsiveness i essential hypertension. *Circulation* 68: 234–240, 1983. doi:10.1161/01.CIR.68.2.234. [PubMed: 6407 [CrossRef: 10.1161/01.CIR.68.2.234]

11. Gribbin B, Pickering TG, Sleight P, Peto R. Effect of age and high blood pressure on baroreflex sensitivity in man. *Circ Res* 29: 424–431, 1971. doi:10.1161/01.RES.29.4.424. [PubMed: 5110922] [CrossRef: 10.1161/01.RES.29.4.424]

12. Hamilton WF, Woodbury RA, Harper HT Jr. Physiologic relationships between intrathoracic, intraspinal and arterial pressures. *JAMA* 107: 853–856, 1936. doi:10.1001/jama.1936.0277037001700 [CrossRef: 10.1001/jama.1936.02770370017005]

13. Hunt BE, Farquhar WB, Taylor JA. Does reduced vascular stiffening fully explain preserved cardiovagal baroreflex function in older, physically active men? *Circulation* 103: 2424–2427, 2001. doi:10.1161/01.CIR.103.20.2424. [PubMed: 11369680] [CrossRef: 10.1161/01.CIR.103.20.2424]

14. Imholz BP, van Montfrans GA, Settels JJ, van der Hoeven GM, Karemaker JM, Wieling W. Continuous non-invasive blood pressure monitoring: reliability of Finapres device during the Valsalva manoeuvre. *Cardiovasc Res* 22: 390–397, 1988. doi:10.1093/cvr/22.6.390. [PubMed: 3224351] [Cros 10.1093/cvr/22.6.390]

15. Kautzner J, Hartikainen JE, Camm AJ, Malik M. Arterial baroreflex sensitivity assessed from pha of the Valsalva maneuver. *Am J Cardiol* 78: 575–579, 1996. doi:10.1016/S0002-9149(96)00370-0. [PubMed: 8806348] [CrossRef: 10.1016/S0002-9149(96)00370-0]

16. La Rovere MT, Bigger JT Jr, Marcus FI, Mortara A, Schwartz PJ; ATRAMI (Autonomic Tone and Reflexes After Myocardial Infarction) Investigators . Baroreflex sensitivity and heart-rate variability in prediction of total cardiac mortality after myocardial infarction. *Lancet* 351: 478–484, 1998. doi:10.1016/S0140-6736(97)11144-8. [PubMed: 9482439] [CrossRef: 10.1016/S0140-6736(97)11144

17. La Rovere MT, Specchia G, Mortara A, Schwartz PJ. Baroreflex sensitivity, clinical correlates, and cardiovascular mortality among patients with a first myocardial infarction. A prospective study. *Circulation* 78: 816–824, 1988. doi:10.1161/01.CIR.78.4.816. [PubMed: 3168190] [CrossRef: 10.1161/01.CIR.78.4.816]

18. Laude D, Elghozi JL, Girard A, Bellard E, Bouhaddi M, Castiglioni P, Cerutti C, Cividjian A, Di Rienzo M, Fortrat JO, Janssen B, Karemaker JM, Lefthériotis G, Parati G, Persson PB, Porta A, Quint Regnard J, Rüdiger H, Stauss HM. Comparison of various techniques used to estimate spontaneous baroreflex sensitivity (the EuroBaVar study). *Am J Physiol Regul Integr Comp Physiol* 286: R226–R2 2004. doi:10.1152/ajpregu.00709.2002. [PubMed: 14500269] [CrossRef: 10.1152/ajpregu.00709.2002

19. Levin AB. A simple test of cardiac function based upon the heart rate changes induced by the Vals maneuver. *Am J Cardiol* 18: 90–99, 1966. doi:10.1016/0002-9149(66)90200-1. [PubMed: 5938917] [CrossRef: 10.1016/0002-9149(66)90200-1]

20. Mattace-Raso FU, van den Meiracker AH, Bos WJ, van der Cammen TJ, Westerhof BE, Elias-Sm S, Reneman RS, Hoeks AP, Hofman A, Witteman JC. Arterial stiffness, cardiovagal baroreflex sensiti and postural blood pressure changes in older adults: the Rotterdam study. *J Hypertens* 25: 1421–1426 2007. doi:10.1097/HJH.0b013e32811d6a07. [PubMed: 17563564] [CrossRef: 10.1097/HJH.0b013e32811d6a07]

21. McIntosh HD, Burnum JF, Hickam JB, Warren JV. Circulatory changes produced by the Valsalva maneuver in normal subjects, patients with mitral stenosis, and autonomic nervous system alterations. *Circulation* 9: 511–520, 1954. doi:10.1161/01.CIR.9.4.511. [PubMed: 13150514] [CrossRef: 10.1161/01.CIR.9.4.511]

22. Monahan KD, Dinenno FA, Seals DR, Clevenger CM, Desouza CA, Tanaka H. Age-associated changes in cardiovagal baroreflex sensitivity are related to central arterial compliance. *Am J Physiol H Circ Physiol* 281: H284–H289, 2001. doi:10.1152/ajpheart.2001.281.1.H284. [PubMed: 11406495] [CrossRef: 10.1152/ajpheart.2001.281.1.H284]

23. Müller A, Morley-Davies A, Barthel P, Hnatkova K, Bauer A, Ulm K, Malik M, Schmidt G. Bivar phase-rectified signal averaging for assessment of spontaneous baroreflex sensitivity: normalization o results. *J Electrocardiol* 45: 77–81, 2012. doi:10.1016/j.jelectrocard.2011.07.010. [PubMed: 2185508 [CrossRef: 10.1016/j.jelectrocard.2011.07.010]

24. Olufsen MS, Tran HT, Ottesen JT, Lipsitz LA, Novak V; Research Experiences for Undergraduate Program . Modeling baroreflex regulation of heart rate during orthostatic stress. *Am J Physiol Regul I Comp Physiol* 291: R1355–R1368, 2006. doi:10.1152/ajpregu.00205.2006. [PubMed: 16793939] [CrossRef: 10.1152/ajpregu.00205.2006]

25. Parati G, Casadei R, Groppelli A, Di Rienzo M, Mancia G. Comparison of finger and intra-arterial blood pressure monitoring at rest and during laboratory testing. *Hypertension* 13: 647–655, 1989.

doi:10.1161/01.HYP.13.6.647. [PubMed: 2500393] [CrossRef: 10.1161/01.HYP.13.6.647]

26. Parati G, Di Rienzo M. Assessing spontaneous baroreflex function: methodological considerations *Clin Sci (Lond)* 103: 89–91, 2002. doi:10.1042/cs1030089. [PubMed: 12095409] [CrossRef: 10.1042/cs1030089]

27. Pettersen KH, Bugenhagen SM, Nauman J, Beard DA, Omholt SW. Arterial stiffening provides sufficient explanation for primary hypertension. *PLOS Comput Biol* 10: e1003634, 2014. doi:10.1371/journal.pcbi.1003634. [PMCID: PMC4031054] [PubMed: 24853828] [CrossRef: 10.1371/journal.pcbi.1003634]

28. Pierce GL, Harris SA, Seals DR, Casey DP, Barlow PB, Stauss HM. Estimated aortic stiffness is independently associated with cardiac baroreflex sensitivity in humans: role of ageing and habitual endurance exercise. *J Hum Hypertens* 30: 513–520, 2016. doi:10.1038/jhh.2016.3. [PMCID: PMC4981524] [PubMed: 26911535] [CrossRef: 10.1038/jhh.2016.3]

29. Rudas L, Crossman AA, Morillo CA, Halliwill JR, Tahvanainen KU, Kuusela TA, Eckberg DL. Human sympathetic and vagal baroreflex responses to sequential nitroprusside and phenylephrine. *Am Physiol Heart Circ Physiol* 276: H1691–H1698, 1999. doi:10.1152/ajpheart.1999.276.5.H1691. [PubM 10330255] [CrossRef: 10.1152/ajpheart.1999.276.5.H1691]

30. Sharpey-Schafer EP. Effects of Valsalva's manoeuvre on the normal and failing circulation. *BMJ* 1 693–695, 1955. doi:10.1136/bmj.1.4915.693. [PMCID: PMC2061457] [PubMed: 14351748] [CrossR 10.1136/bmj.1.4915.693]

31. Smith ML, Beightol LA, Fritsch-Yelle JM, Ellenbogen KA, Porter TR, Eckberg DL. Valsalva's maneuver revisited: a quantitative method yielding insights into human autonomic control. *Am J Phys Heart Circ Physiol* 271: H1240–H1249, 1996. doi:10.1152/ajpheart.1996.271.3.H1240. [PubMed: 8853364] [CrossRef: 10.1152/ajpheart.1996.271.3.H1240]

32. Stefanadis C, Stratos C, Vlachopoulos C, Marakas S, Boudoulas H, Kallikazaros I, Tsiamis E, Toutouzas K, Sioros L, Toutouzas P. Pressure-diameter relation of the human aorta. A new method of determination by the application of a special ultrasonic dimension catheter. *Circulation* 92: 2210–221 1995. doi:10.1161/01.CIR.92.8.2210. [PubMed: 7554204] [CrossRef: 10.1161/01.CIR.92.8.2210]

33. Thrasher TN. Unloading arterial baroreceptors causes neurogenic hypertension. *Am J Physiol Reg Integr Comp Physiol* 282: R1044–R1053, 2002. doi:10.1152/ajpregu.00431.2001. [PubMed: 1189360 [CrossRef: 10.1152/ajpregu.00431.2001]

34. Tiecks FP, Lam AM, Matta BF, Strebel S, Douville C, Newell DW. Effects of the Valsalva maneuv on cerebral circulation in healthy adults. A transcranial Doppler study. *Stroke* 26: 1386–1392, 1995. doi:10.1161/01.STR.26.8.1386. [PubMed: 7631342] [CrossRef: 10.1161/01.STR.26.8.1386]

35. Westerhof BE, Gisolf J, Stok WJ, Wesseling KH, Karemaker JM. Time-domain cross-correlation baroreflex sensitivity: performance on the EUROBAVAR data set. *J Hypertens* 22: 1371–1380, 2004. doi:10.1097/01.hjh.0000125439.28861.ed. [PubMed: 15201554] [CrossRef: 10.1097/01.hjh.0000125439.28861.ed]

36. Zuern CS, Eick C, Rizas KD, Bauer S, Langer H, Gawaz M, Bauer A. Impaired cardiac baroreflex

sensitivity predicts response to renal sympathetic denervation in patients with resistant hypertension. *Coll Cardiol* 62: 2124–2130, 2013. doi:10.1016/j.jacc.2013.07.046. [PubMed: 23973686] [CrossRef: 10.1016/j.jacc.2013.07.046]

Figures and Tables

Fig. 1.

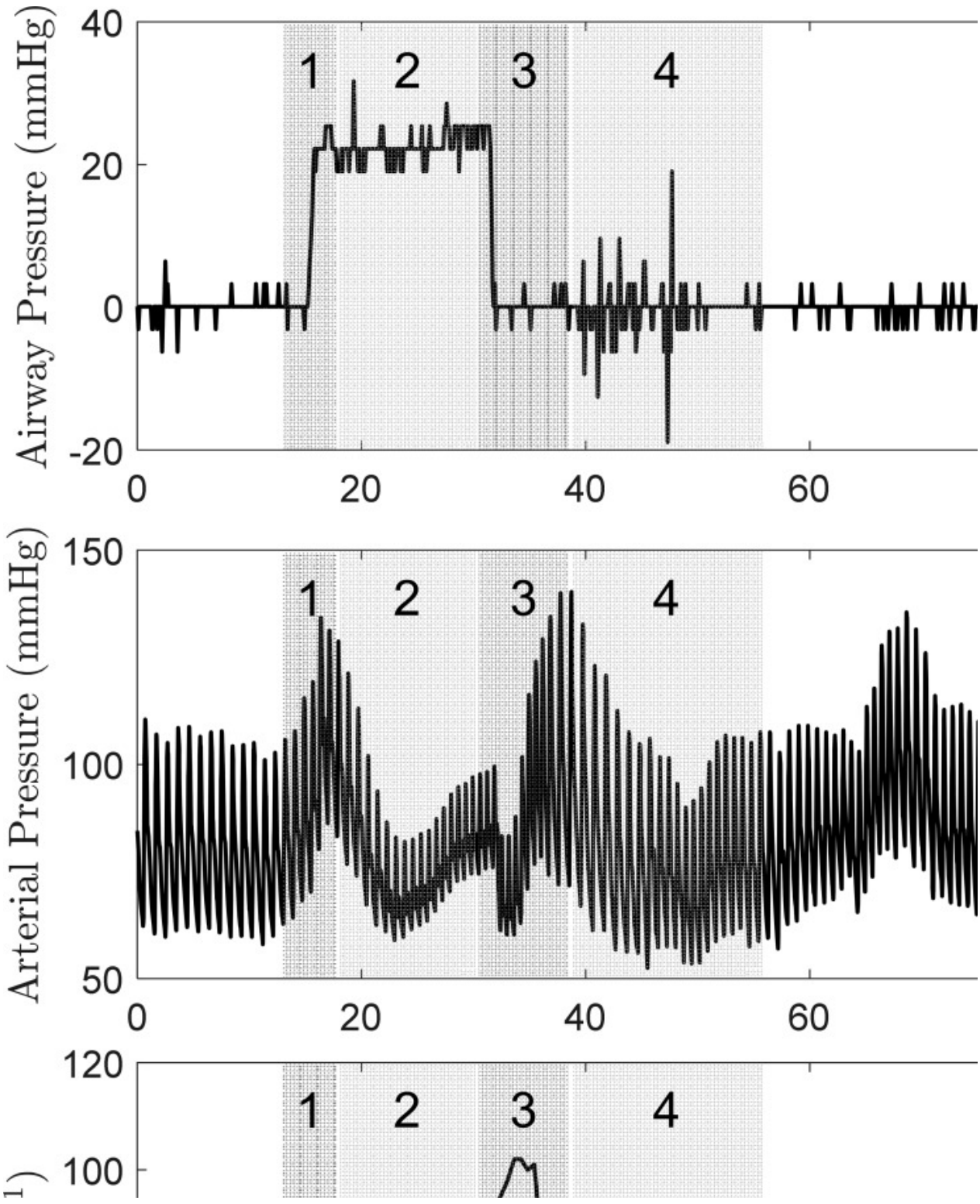

Arterial pressure and heart rate response to Valsalva maneuver. Measured data are shown for *subject 4* (female, 4 yr old). *Top*: measured expiratory pressure; maintained an ~20-mmHg pressure during the Valsalva period between approximately times $t = 15$ and 31 s. *Middle*: arterial pressure measured by the Finometer device.

Bottom: measured heart rate (HR) over the observed time course. The four phases described in the text (phases 1–4) of the baroreflex are indicated on the graphs.

Fig. 2.

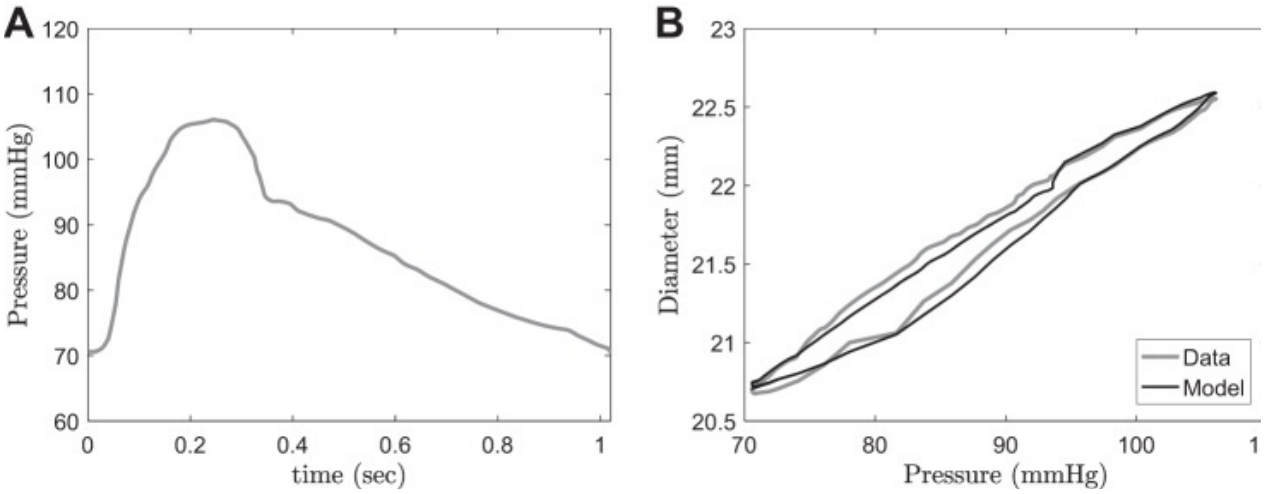

Arterial diameter-pressure relationship. Arterial pressure and aortic diameter time courses obtained over the cardiac cycle for a normal control subject were obtained from the study of Stefanadis et al. (32; Fig. 7 therein). *A* arterial pressure wave. *B*: pressure-diameter loop for the cardiac cycle. The model of *Eq. 3* is fit to the data yielding parameter estimates $\mu = 2.1$ s·mmHg, $k = 0.505$ mmHg/mm^2, and $D_o = 12.35$ mm, where the parameter represents an effective viscosity of the vessel wall and k and D_o determine the stiffness of the vessel.

Table 1.

Physiologically based model parameters

Name	Explanation	Value	Units
μ	Vessel wall viscosity parameter	2.1	s·mmHg
k'	Vessel wall elasticity parameter	202	mmHg
D'	Vessel wall mechanics parameter	0.6175	Unitless
τ_s	Time constant of afferent adaptation	30*	s
δ_o	Afferent firing sensitivity constant	0.4965	Unitless
a	Afferent fiber activation rate	0.0651	s^{-1}
b	Afferent fiber deactivation rate	0.2004	s^{-1}
f_0	Afferent firing rate factor	300	s^{-1}
H_0	Heart rate parameter	28	min^{-1}
H_1	Heart rate parameter	156	min^{-1}
f_{SN}	Sympathetic tone activation rate	Adjustable	s^{-1}
f_1	Sympathetic tone inhibition rate	Adjustable	Unitless
g	Relative aortic/carotid strength	Adjustable	Unitless

*Results not sensitive to the value of the parameter.

Fig. 3.

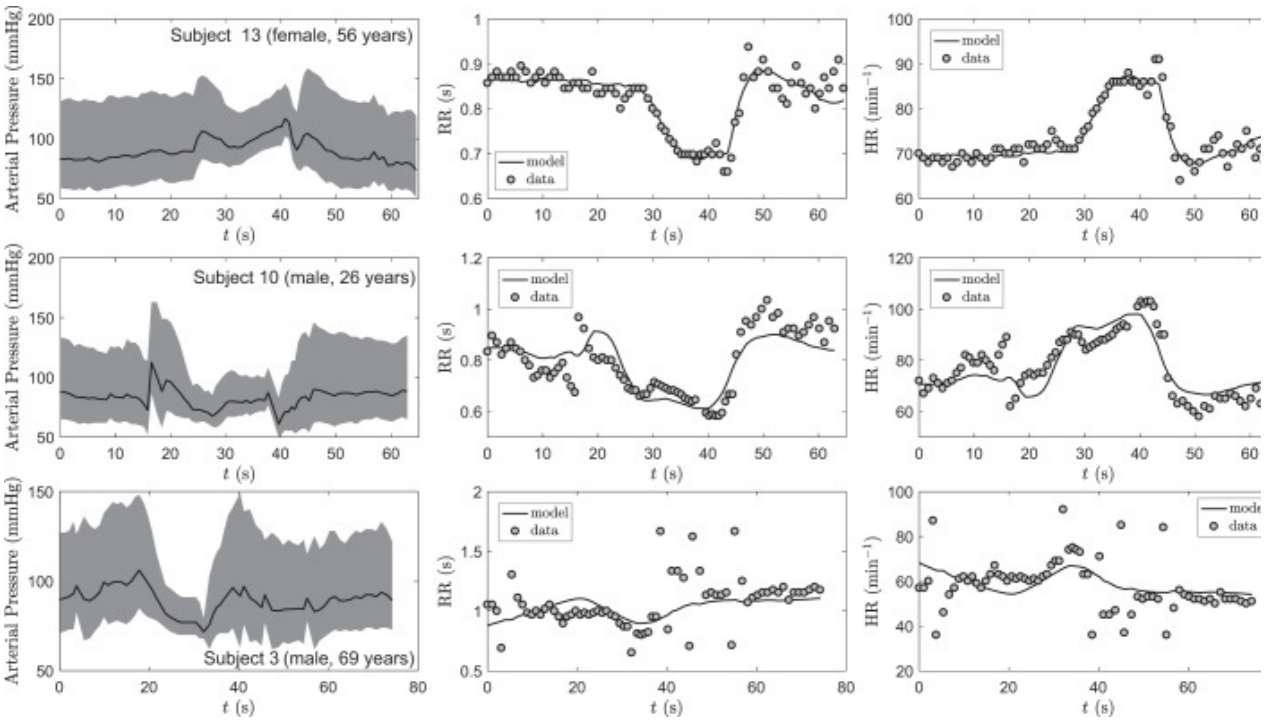

Arterial pressures, R-R intervals [RR(*t*)], and heart rate (HR) responses to Valsalva for three representative subjects. *Top*: measured data and linear filter model of Eqs. 1 and 2 fit for *subject 13*, the subject with the best fi of the model to the RR(*t*) data. *Middle*: the fit to data from *subject 10* shows the median error value. *Bottom*: the fit to data from *subject 3* shows the highest error (worst fit) for the population. The estimated model parameters for these subjects are as follows: *subject 13*, time constant (τ) = 2.05 s, linear filter offset (R_o) = 0.459 s^{-1}, gain (α) = 5.42 ms/mmHg; *subject 10*, τ = 3.14 s, R_o = 0.405 s^{-1}, α = 6.56 ms/mmHg; and *subject 3*, τ = 10.9 s, R_o = 0.286 s^{-1}, α = 15.7 ms/mmHg.

Table 2.

Summary statistics for baroreflex functional analysis

	Female	Male	Combined	*P* Value
Demographics				
n	14	13	27	
Age	35.6 ± 16.5	44.5 ± 21.4	39.9 ± 19.2	0.253
Systolic pressure, mmHg	113 ± 10.2	118 ± 14.2	116 ± 12.3	0.278
Diastolic pressure, mmHg	74 ± 8.12	71.7 ± 7.65	73.1 ± 7.87	0.376
Linear filter parameters				
α, ms/mmHg	9.84 ± 4.59	9.84 ± 4.49	9.84 ± 4.45	0.997
τ, s	2.89 ± 2.47	5.07 ± 3.57	3.94 ± 3.19	0.0759
Physiological model parameters				
f_{SN}, s^{-1}	0.041 ± 0.024	0.036 ± 0.030	0.038 ± 0.027	0.656
f_1	0.0046 ± 0.0025	0.0041 ± 0.0027	0.0043 ± 0.0026	0.713
g	0.66 ± 0.16	0.54 ± 0.22	0.59 ± 0.20	0.318

Values are means ± SD; *n* = no. of subjects. Here, α, gain; τ, time constant; f_1, sympathetic tone inhibition rate; f_{SN}, sympathetic tone activation rate; *g*, relative aortic/carotid strength.

Fig. 4.

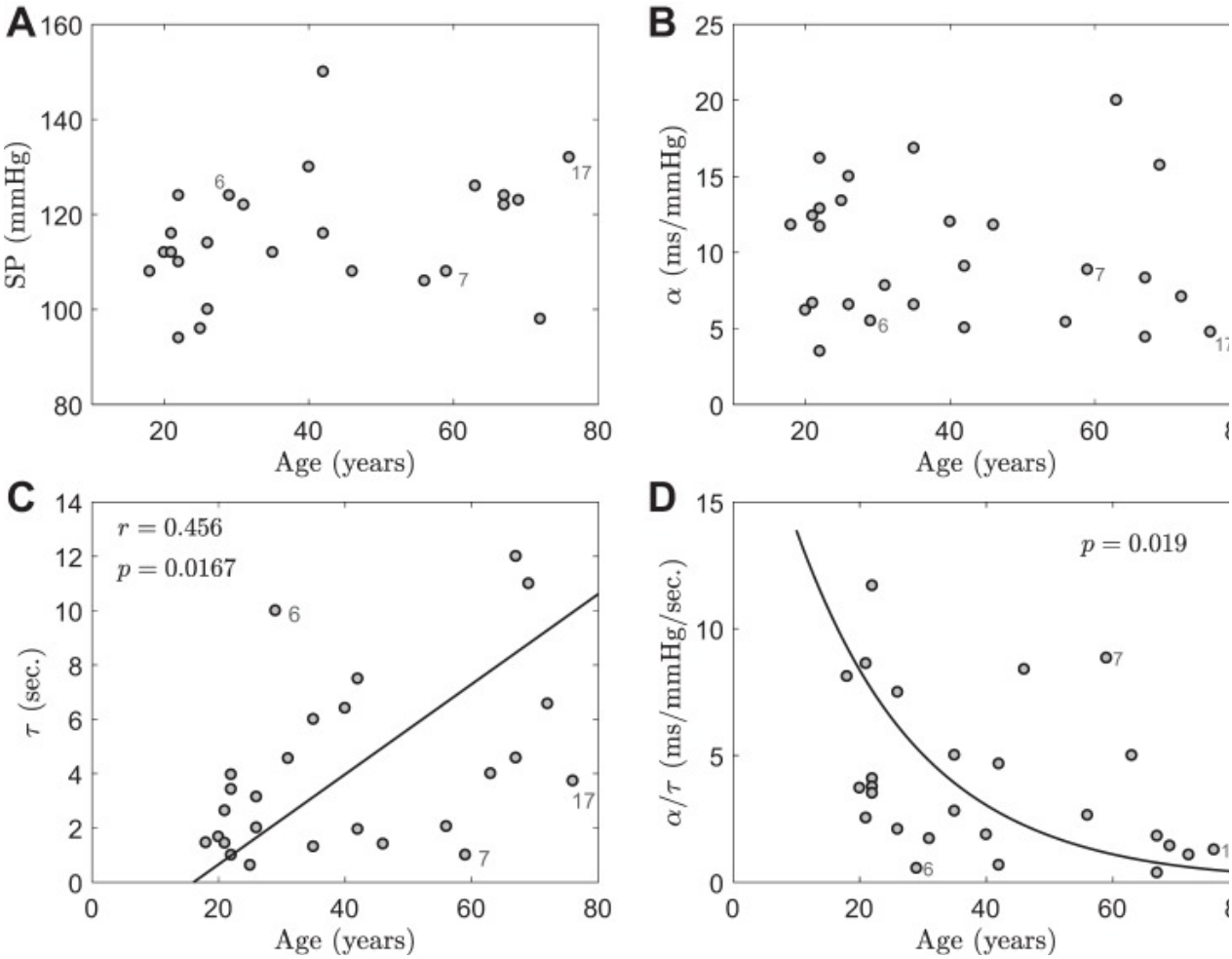

Relationships among linear filter parameters and subject characteristics. *A*: plot of systolic pressure (SP) vs. age reveals no relationship between these metrics. *B*: plot of estimated filter gain (α) vs. age reveals no relationship between the metrics. *C*: plot of filter time constant (τ) vs. age reveals a statistically significant increase in τ with age, with correlation coefficient and *P* value indicated in plot. *D*: estimated gain divided by time constant (α/τ) is plotted as a function of age, revealing a decreasing trend. These data are fit to a decreasing exponential function $a/\tau \sim \exp(-\text{age}/a)$, with $a = 19.7$ yr. The major outliers (*subjects 6*, *7*, and *17*) from the plots in *C* and *D* are indicated in the figure.

Fig. 5.

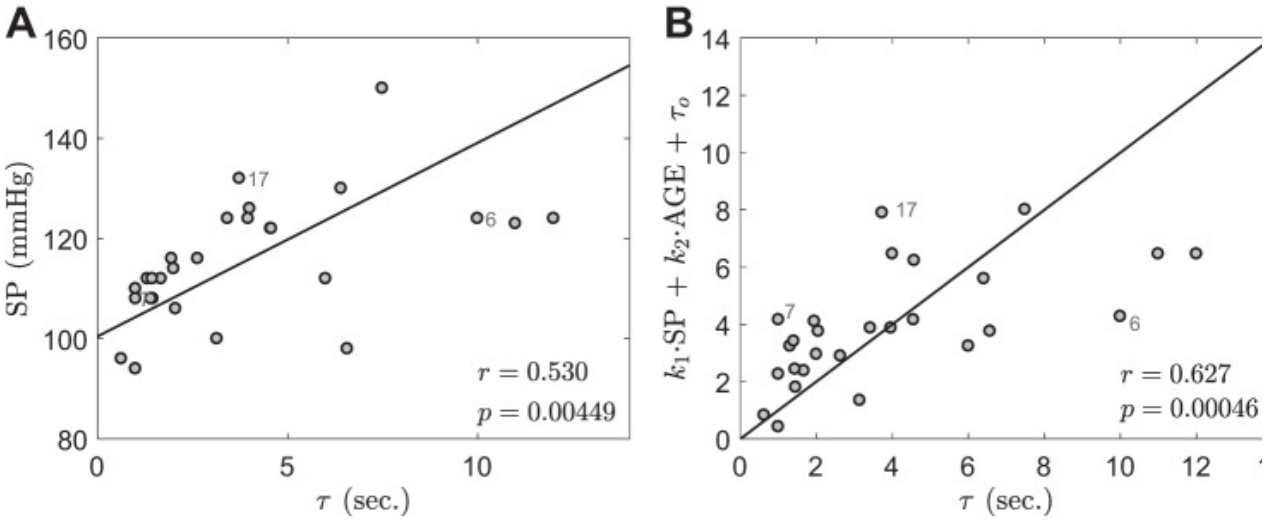

Predictive relationships associated with filter response time. *A*: systolic pressure (SP) tends to increase in proportion to response time (τ), with $P < 0.01$. *B*: multiple regression for $\tau = k_1 \cdot \mathrm{SP} + k_2 \cdot \mathrm{AGE} + \tau_0$. Estimated regression coefficients are $k_1 = 0.115$ s/mmHg, $k_2 = 0.0575$ s/yr, and $\tau_0 = -11.6$ s. The major outliers from the plots in Fig. 4 are indicated.

Fig. 6.

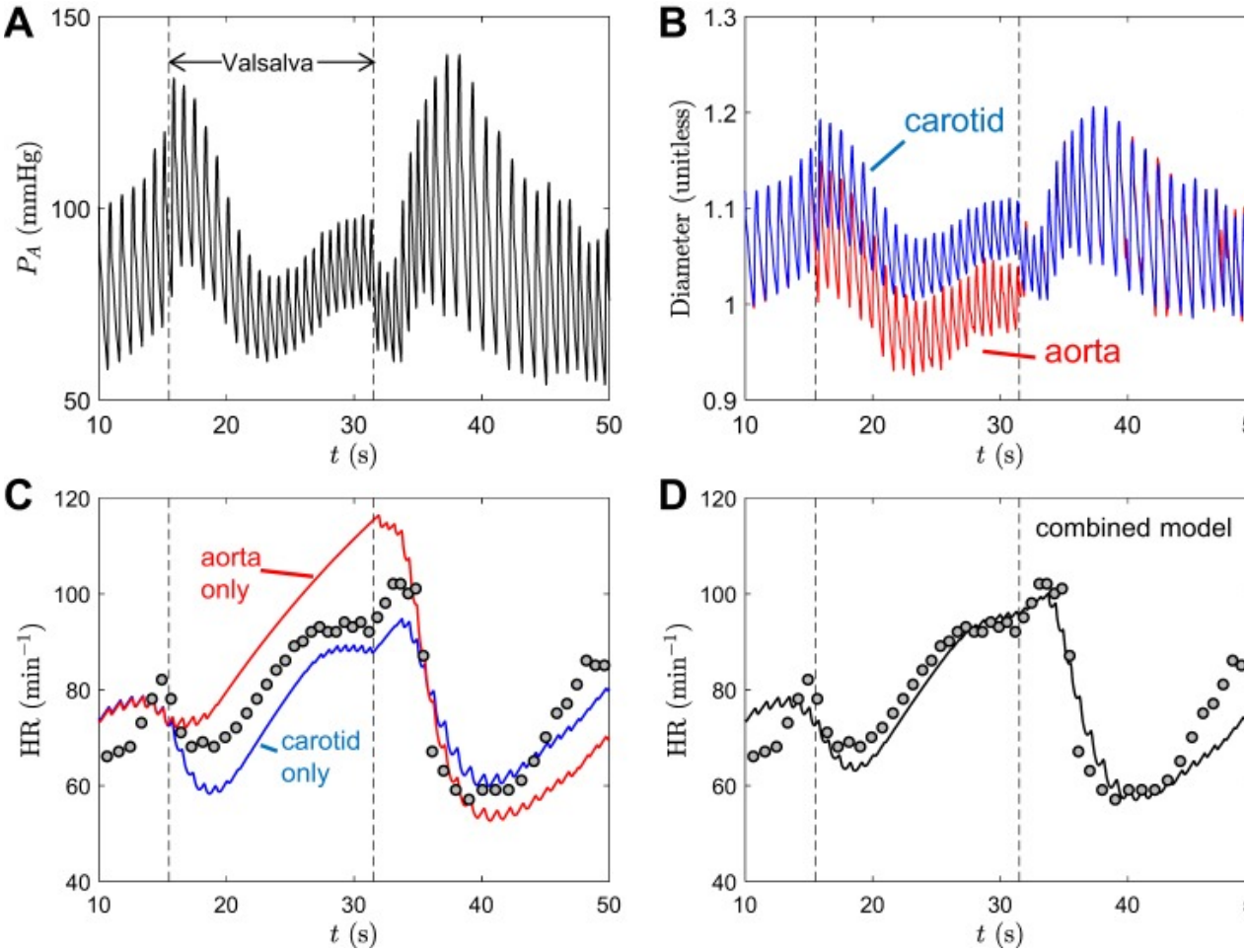

Analysis of baroreflex response using physiologically based model. *A*: arterial pressure (P_A) measured by Finometer for *subject 4*. *B*: diameters for the aorta and carotids are predicted from Eq. 4. The relative (unitless) diameters are identical for the period preceding the Valsalva. During the Valsalva, the relative aortic diameter is lower than that of the carotids because of the external pressure acting to compress the vessels in the thoracic cavity. *C*: the heart rate (HR) response predicted by the physiologically based model is compared with the measure data for the aortic-only and carotid-only versions of the model. *D*: the heart rate response predicted by the physiologically based model is compared with the measured data for the combined (aortic + carotid) version of the model. Values for adjustable model parameters are as follows: sympathetic tone activation rate (f_{SN}) = 0.0365 s^{-1}, sympathetic tone inhibition rate (f_1) = 0.0052, and relative aortic/carotid strength (g) = 0.35. The window over which the Valsalva maneuver is executed is indicated by dashed lines in all panels.

Fig. 7.

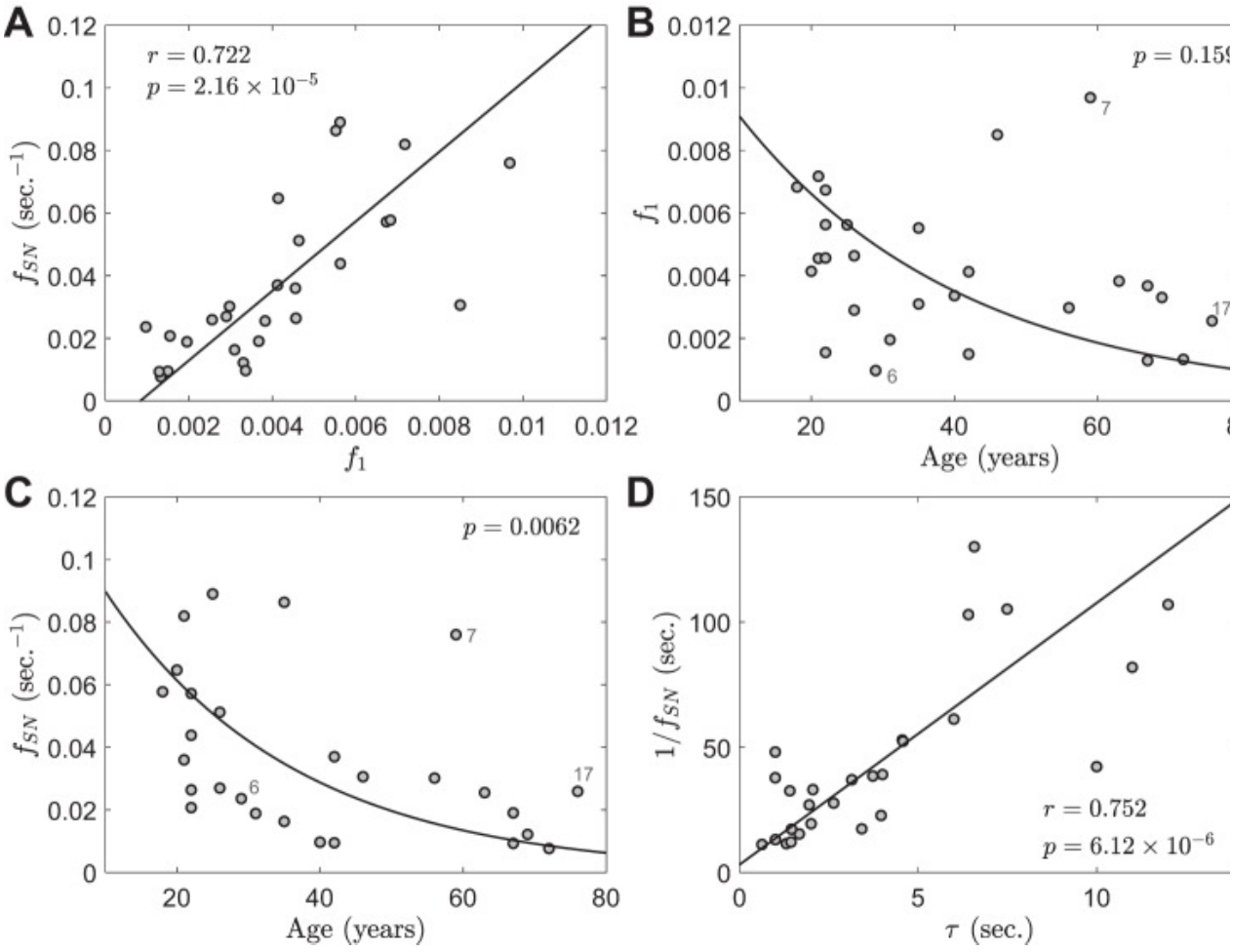

Relationships among linear filter parameters, physiologically based model parameters, and subject characteristic *A*: plot of estimated sympathetic tone activation rate (f_{SN}) vs. sympathetic tone inhibition rate (f_1) for the physiologically based model (representing rates of increase and decrease in sympathetic tone) reveals a high degree of correlation. *B*: estimated f_1 as a function of age is matched to a decaying exponential $f_1 \sim \exp(-\text{age}/a)$ with $a = 31.5$ yr. *C*: estimated f_{SN} as a function of age is matched to a decaying exponential $f_{SN} \sim \exp(-\text{age}/a)$, with $a = 26.4$ yr. The exponential decrease is shown to be statistically significant for f_{SN} ($P < 0.01$), but not for f These trends are closely related to the observed correlation between the filter response time (τ) and age illustrate in Fig. 4. *D*: estimated τ (from the linear filter analysis) is closely correlated with $1/f_{SN}$, estimated using the physiologically based model.